Detection of Oil on and Under Ice:

Phase III

Evaluation of Airborne Radar System Capabilities in Selected Arctic Spill Scenarios

DICKINS

BOISE STATE UNIVERSITY

July 2008

Detection of Oil on and Under Ice:

Phase III

Evaluation of Airborne Radar System Capabilities in Selected Arctic Spill Scenarios

Final Technical Report

July 14, 2008

United States Department of Interior
Minerals Management Service
Contract Number MO7PX13062

Submitted by:

DF Dickins Associates Ltd.
David Dickins
info@dfdickins.com

Boise State University
John Bradford and Leah Steinbronn
johnb@cgiss.boisestate.edu

DISSEMINATION AND APPLICATION OF RESULTS

Findings from this project are publicly available. The full report will be posted on the MMS website http://www.mms.gov/tarprojects/588.htm. The authors will produce a manuscript for peer-reviewed journal publication with key findings. Ongoing research benefiting from this study includes the Joint Industry Program on Oil Spill Response for Arctic and Ice-covered Waters (2006-2009).

DISCLAIMER

U.S. Minerals Management Service (MMS) staff has reviewed this report for technical adequacy according to contractual specifications. The opinions, conclusions and recommendations contained in this report are those of the author and do not necessarily reflect views and policies of the U.S. MMS. The mention of any trade name or commercial product in this report does not constitute an endorsement for use by the U.S. MMS. Finally this report does not contain any commercially sensitive, classified, or proprietary data release restrictions and may be freely copied and widely distributed.

SUMMARY, CONCLUSIONS AND RECOMMENDATIONS

Background and Objectives

The lack of any practical operational remote sensing system to detect oil in ice was identified as a priority research gap in Dickins (2004). The accelerating level of interest in Arctic oil and gas exploration was demonstrated in the bid values offered in recent lease sales in the Alaskan OCS Region. The need for proven and reliable systems to detect oil trapped in a range of ice conditions remains at the forefront of continued efforts to advance Arctic spill response capabilities, for example through the international joint industry project under way in Norway (Sorstrom 2007).

Under continued Minerals Management Service (MMS) sponsorship, the development of oil-in-ice detection systems has made significant progress over the past four years through a series of related projects involving tank and basin trials, field tests and, most recently through this study, model simulations of radar detection performance in a range of ice conditions. MMS-supported achievements to date in this area are summarized briefly as follows:

1. Phase I: A test basin experiment in November 2004 demonstrated the potential for off-the-shelf ground penetrating radar (GPR) systems and an ultra-sensitive ethane sensor to detect oil trapped under model sea ice (Dickins et al., 2005). www.mms.gov/tarprojects/517.htm

2. A follow-on series of studies (March to July 2005), focused on further developing the radar technology into a reliable and more "user friendly" spill response tool. Tasks in this program included:
   - Evaluating available hardware solutions for multi-polarization GPR data;
   - Field testing over up to 2 meters of sea ice at temperatures down to –20°C without oil (Prudhoe Bay, April 2005);
   - Developing improved radar-processing software for the oil-in ice-problem (Bradford, 2005). This software is now incorporated as part of an operational GPR system deployed by ACS in 2008.

3. Phase II: MMS in conjunction with six other government and industry partners funded a field spill under ice on Svalbard in March 2006, carried out jointly by DF Dickins, SINTEF, and Boise State University. This project demonstrated the ability to detect oil under 65 cm of relatively warm ice (2006 was an unusually mild winter) from the surface with commercially available GPR systems. With climatic conditions at the time of the experiment, the radar system used in 2006 lacked the power to penetrate the sea ice when flown at low altitude by helicopter. Subsequent modeling results reported in this study showed that airborne profiling of oil trapped beneath the ice has a high probability of succeeding with colder ice sheets more likely to be encountered for example in the Beaufort Sea in mid winter.

4. SINTEF JIP Project 5 - Remote Sensing: Although not a principal objective at the time, the 2006 airborne tests demonstrated that the existing GPR can provide an accurate profile of the ice surface and snow topography. These results have direct applications to the scenario of surface oil on ice or frozen ground buried by snow. In order to confirm these findings and validate the model simulations developed in this study, the GPR was retested in an airborne mode on Svalbard in April 2008 over snow-covered oil on the ice surface. Costs for this trial relied on a sharing of resources between SINTEF and MMS. Successful results from the latest field trials are covered in this report (6.3.1).

The scope of the current study was developed as a response to several key recommendations following the 2006 Svalbard trials (Dickins et al. 2006):

- Model the expected radar response to different oil in ice and oil in snow scenarios.
- Evaluate the need to develop and test an operational airborne radar system capable of detecting oil under ice and snow of different composition and thickness.

The current study was designed around the following main tasks:

- Review available systems and potential sources of necessary hardware that could provide a basis for future higher-powered airborne systems if this proves necessary to achieve successful detection from a helicopter platform.
- Assess the necessary timelines and level of funding required to develop a prototype airborne system with sufficient power to map the ice/water interface from a helicopter (only if the model results indicate that existing off-the-shelf systems are unable to achieve this objective)
- Use existing Boise State GPR modeling software to carry out computer simulations, for a variety of oil under-ice and oil trapped-in-ice scenarios.
- Assess the future potential of off-the-shelf GPR systems to map oil on top of solid ice, buried under varying thicknesses of snow.

Results

The overall results from this study are very promising in that they indicate that airborne GPR using currently available systems is capable of detecting and mapping oil in ice over a broad operational time window from early to late winter, typically November to April in the Beaufort Sea area. There are still challenges in detecting oil early in the winter with thin, high salinity ice sheets (October) and in the spring (May/June) with warm thick ice having a high volume of liquid brine.

Higher-powered radar systems would need to be developed to cover the beginning and end phases of the ice cycle. Detection of trapped oil is not as critical during these periods as the oil will naturally surface through the porous ice and provide a clear visual indication of the presence of residual trapped oil.

The overlap period where radar detection is questionable and the oil is still completely contained within the ice (not visible on the surface) is estimated at approximately one month out of the year: one to two weeks in late October and early November, and up to two weeks in the first half of May.

For all scenarios tested, numerical modeling results indicate that GPR methods can detect oil films as long as adequate energy reaches the ice/water interface. The minimum oil film detection limit appeared to be roughly 2 cm in the original numerical models. Testing in earlier phases of the GPR development (at CRREL in 2004 and on Svalbard in 2006) confirmed that this level of resolution was possible with actual ice sheets in cold basins and in the field. Local ice conditions (including salinity and temperature) may still be a limiting factor and further tests are necessary to determine how consistently this level of resolution can be achieved.

The primary factor limiting signal penetration is brine volume. Brine volume is a function of both temperature and salinity. Brine volume increases with temperature and there is a critical point at around -5°C at which electric conductivity increases rapidly and radar signal penetration is severely limited. Late in the season, thick warm ice prevents effective signal penetration. In the early season, the young ice tends to be relatively warm and have high salinity, however since the ice is thin it may still be possible to penetrate to the ice/water interface.

This effect is summarized in the graph below where radar amplitude from the ice/oil/water interface is plotted as a function of oil thickness for typical Beaufort Sea ice conditions from November through April. The strongest signal is seen in January and February, while April produces the weakest signal. November, December and March are intermediate in terms of signal strength. Note that the signal amplitude varies by three orders of magnitude depending on ice conditions, but that the amplitude trend as a function of oil thickness is consistent.

Placing the numerical modeling results in the context of making measurements from an airborne platform, it appears that oil under cold, mid-winter ice in January and February could be effectively surveyed from an airborne platform at a height of 20 meters using existing equipment. Results of recent tests just completed in April, 2008, in cooperation with SINTEF, showed that a commercial radar system could consistently image the ice water interface under 80 cm thick cold ice (equivalent to late December or January in the Beaufort Sea).

The signal to noise ratio would need to be increased by a factor of 100 to reliably image the ice/oil/water interface under marginal conditions (represented by the periods November to December and March to April). Achieving consistent detection during early and late winter will likely require design and construction of new, purpose built radar hardware of higher power.

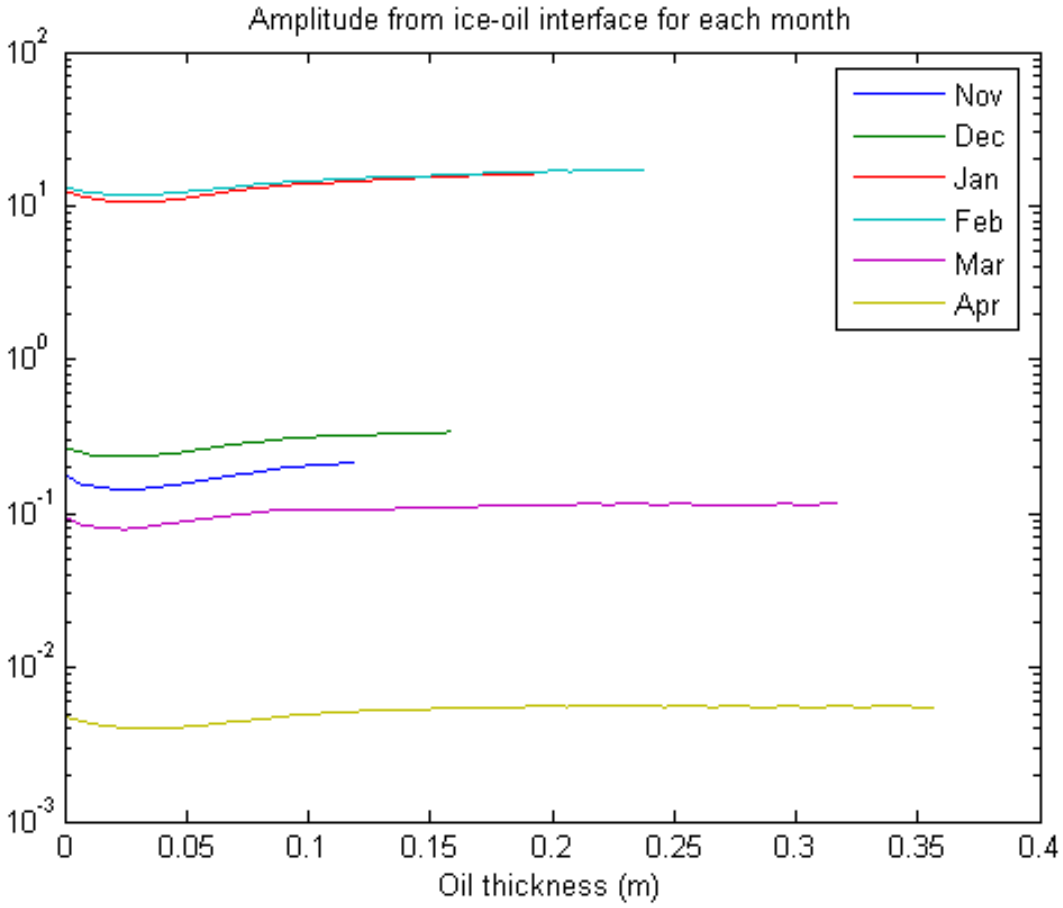

An important finding is that despite the large changes in reflection strength amplitude, changes in other measurable properties of the radar signal such as phase (wave shape) are largely independent of ice conditions. For example, in the plot below, the instantaneous phase of the received signal is plotted for all months as a function of oil thickness. For films between 2 and 12 cm thick, a large phase anomaly is introduced, and this response is nearly independent of ice conditions. This result is encouraging and consistent with field observations from the Svalbard field test in 2006. Overall, detection of oil in and under sea ice appears promising under a broad range of ice conditions through detailed measurements of reflected wave properties.

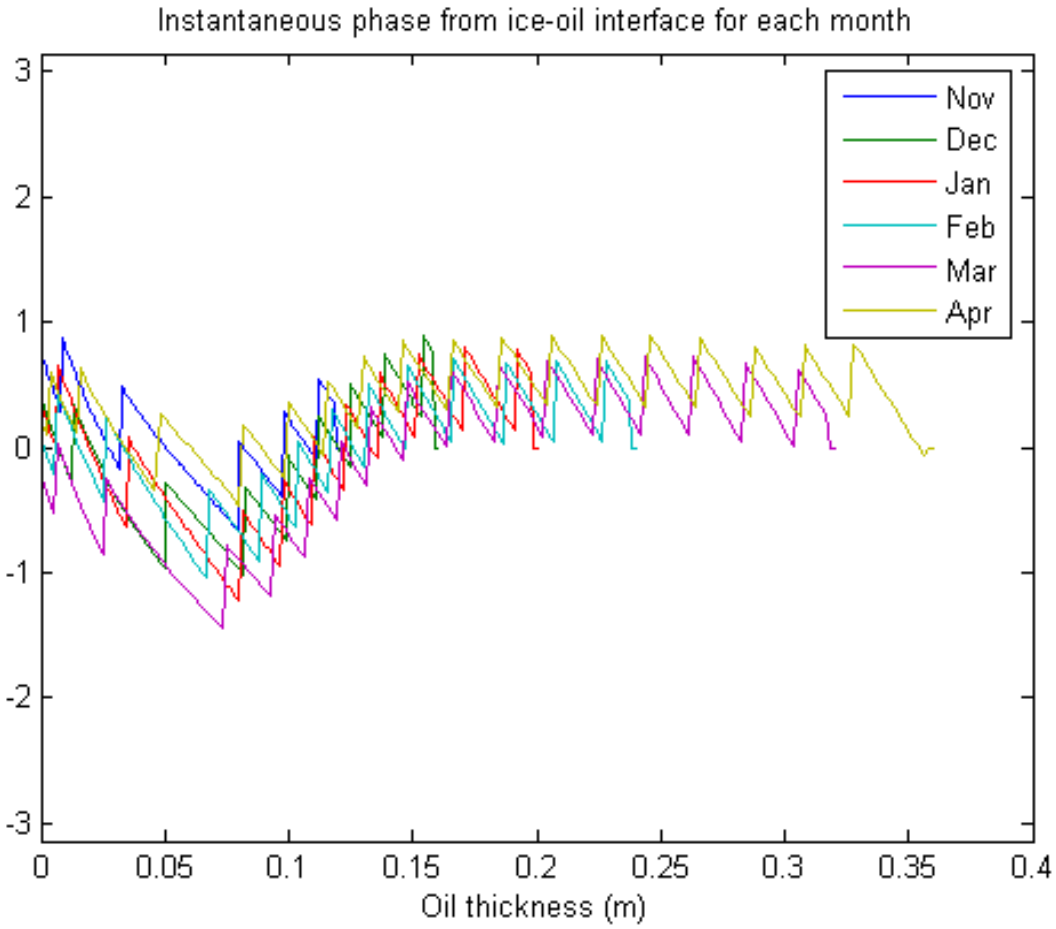

The following matrix shows the expected range of surface and airborne applicability of GPR detection methods based on the modeling results from this study and drawing on findings from the 2004 basin tests at CRREL and the 2006 and (just completed) 2008 field experiments at Svalbard. This chart shows that the existing commercial GPR systems are capable of airborne imaging oil under ice or trapped within the ice sheet from November to March (representing 55% of the ice season between early October and early July). The most reliable months for detection are January and February with results in November, December and March depending on the internal brine volume of the ice (combination of salinity and temperature). Consistent imaging results in these months will require the development of higher-powered airborne radar systems and/or a corresponding improvement in signal to noise ratios.

The current generation of commercial GPR's operating on the ice surface is capable of reliably imaging oil under ice or trapped within the ice sheet, in a Beaufort Sea environment from November to April.

Range of Applicability for GPR Detection of Oil in Ice				
Ice Age	**Ice Thickness (cm)**	**Oil Pool Depth (cm)**	**Oil Under Ice or as a Trapped Layer**	
			Airborne Radar	**Surface Radar**
Early Winter Ice (October to December) - 30% of the ice season				
New or nilas	<10	N/A		
Young	10 – 30	2 - 3		
Thin First-year	30-70	3 - 7		
Winter Ice (January to February) - 25% of the ice season				
Medium First-year	70 – 120	7 - 12		
Thick First-year	120 – 200	12 - 21		
Late Winter Ice (March to April) - 25% of the ice season				
Thick First-year	120 - 200	12-21		
Spring and Summer Ice (May to June) - 20% of the ice season				
First-year ice	Highly variable	N/A		
Deformed Ice (any time of year)				
Rafted ice, rubble, ridges	30 cm to 10 m+	Highly variable cm to m		

	Detection considered highly unlikely due to warm, saline ice and lack of a defined oil layer. Ice too thin for surface operations.
	Detection possible in the future with higher-powered systems. Results uncertain, due to poorly defined oil layer in thin ice.
	Detection possible with existing systems but dependent on ice salinity and temperature. Consistent and reliable detection will require higher-powered radar systems or an improvement in signal to noise ratios.
	Consistent and reliable detection expected, based on knowledge gained at CRREL (2004) and Svalbard (2006 and 2008).

For oil on the ice trapped beneath snow, existing GPR systems are capable of imaging the oil layer in an airborne mode through the entire ice season. The model results for oil –under-snow scenarios in this study indicated a positive mapping response in every situation considered. These findings were recently validated and confirmed in airborne tests over an actual spill on the ice at Svea, Svalbard in a joint program with SINTEF.

Largely as a result of the progress made over the past four years through MMS-sponsored research, GPR can now be considered as an operational tool to detect oil in a wide range of snow and ice conditions.

Recommendations

Based on the findings of this study, a number of recommendations are made to further advance our understanding of the capabilities of GPR under different snow, ice and oil conditions throughout the winter season. The intent of continuing this development work is to create the basic knowledge base that will result in further operational tools based on GPR technology. The recent (2007) commissioning of an operational GPR unit with a core of trained responders on the North Slope is a positive step in that direction.

Future recommended study areas include:

1. Prototyping (leading to the development of actual hardware for flight testing) a higher-powered airborne system to handle warmer and/or higher-salinity ice sheets often encountered early and late in the ice season;

2. Carrying out further field tests of both the existing hardware and potentially a higher-powered system to take full advantage of any further spills planned for solid ice on Svalbard in 2009 through the SINTEF JIP. The intent here would be to conduct a second spill under ice, similar to the one undertaken in 2006 but aiming for colder ice to fully demonstrate the radar performance potential under Arctic winter conditions (the 2006 trials took place during a period of extremely mild temperatures);

3. Converting the model results presented here into a simple responder's guide to indicate when a decision to use GPR on an actual spill would most likely give positive results in both surface and airborne applications.

It is important to recognize that the radar response to oil on, in, or under ice depends on a variety of factors including ice temperature, salinity, thickness, the electrical properties of the oil, and the oil layer thickness. The modeling tools developed as part of this project produce realistic simulations of field conditions. This is in part because actual measured values, specifically ice temperature and salinity, were used primary inputs to the model. Based on the same methods and analytical tools, models can now be constructed and run in a matter of a few hours for any specific scenario. With further software development, this modeling process could become part of the operational decision to use GPR in any given set of circumstances.

A recommended strategy for deployment of GPR in during an actual spill then becomes:

1) Collect a sample of the spilled oil if available, and measure its dielectric permittivity. This can be done rapidly using a time-domain reflectometry probe or the GPR system itself.
2) Acquire ice thickness, temperature and salinity profiles from the spill area.
3) Run numerical model with varying oil thickness to verify applicability of GPR to particular spill conditions and predict expected response.

Following this protocol will enable operators to deploy the system appropriately and maximize the likelihood of successful oil detection.

Table of contents page

1. Introduction and Background

A concerted Canadian research effort in the 1980's, sponsored by industry and government, analyzed and tested a variety of technologies to detect oil in or under solid ice, including radar, electromagnetic and acoustics (e.g. Butt et al., 1981; Goodman and Fingas, 1985; Jones and Kwan, 1982). Dickins (2000) summarized the state of the art based on historical work. Results at the time were mixed and included contradictory and ambiguous tests with radar, now largely attributed to the relatively crude signal processing software available at the time. The lack of any practical operational remote sensing system to detect oil in ice continued to be identified as a priority research gap in for example Dickins (2004).

The accelerating level of interest in Arctic oil and gas exploration was demonstrated in the overwhelming response to recent lease sales in the Alaskan OCS Region. The need for proven and reliable systems to detect oil trapped in a range of ice conditions remains at the forefront of continued efforts to advance Arctic spill response capabilities, for example through the international joint industry project under way in Norway (Sorstrom 2007).

Under continued Minerals Management Service (MMS) sponsorship, the development of oil and ice detection systems has made significant progress over the past four years through a series of related projects involving tank and basin trials, field tests and, most recently (this study), model simulations of detection performance in a range of ice conditions. MMS work to date in this area is summarized as follows:

1. Phase 1: A test basin experiment in November 2004 demonstrated the potential for off-the-shelf ground penetrating radar (GPR) systems and an ultra-sensitive ethane sensor to detect oil trapped under model sea ice (Dickins et al., 2005). www.mms.gov/tarprojects/517.htm

2. A follow-on study (March to July 2005), focused on further developing the radar technology into a reliable and more "user friendly" spill response tool. Tasks in this program included:
   - Evaluating available hardware solutions for multi-polarization GPR data;
   - Field testing over up to 2 meters of sea ice at temperatures down to –20°C without oil (Prudhoe Bay, April 2005);
   - Developing improved radar-processing software for the oil-in ice-problem (Bradford, 2005). This software is incorporated as part of an operational GPR system deployed by ACS in 2007.

3. Phase II: A field spill under ice took place near Sveagruva, Svalbard in March 2006, carried out jointly by DF Dickins, SINTEF, and Boise State (funded by MMS in conjunction with six other government and industry partners). This project demonstrated the ability to detect oil under 65 cm relatively warm ice (2006 was an unusually mild winter) from the surface with commercially available ground penetrating radar (GPR) systems. With climatic conditions at the time of the experiment, the GPR lacked the power to penetrate the sea ice when flown at low altitude by helicopter. Subsequent modeling results reported in this study showed that airborne profiling of oil trapped beneath the ice has a high probability of succeeding with colder ice sheets more likely to be encountered for example in the Beaufort Sea in mid winter.

4. SINTEF JIP Project 5 - Remote Sensing: Although not a principal objective at the time, the 2006 airborne tests also demonstrated that the existing GPR can provide an accurate profile of the ice surface and snow topography. These results have direct applications to the scenario of surface oil on ice or frozen ground buried by snow. In order to confirm these findings and validate the model simulations discussed here (Chapter 6), the GPR was retested at the same location on Svalbard in April 2008 over snow-covered oil on the ice surface. Preliminary results from those trials are described in Section 6.3.1.

2. State of Knowledge

The following sections summarize the state of knowledge with regard to oil and ice properties affecting spill behavior in different situations, including:

- Oil spreading under ice and on the surface with snow
- Evolution and seasonal variations in trapped brine affecting radar signal penetration and oil migration
-

An understanding of likely oil behavior under different conditions of ice and snow is essential to constructing realistic scenarios for evaluating GPR performance (Chapter 5).

2.1 Oil Spreading under Solid Ice

Even large spills (tens of thousands of barrels) of crude oil underneath or on top of solid (or fast ice) will usually be contained within hundreds of meters from the spill source. Except in unusual circumstances with high under-ice currents, the spilled oil will not move any significant distance from its initial point of contact with the ice underside.

Natural variations in first-year ice thickness provide huge natural "reservoirs" to effectively contain oil spilled underneath the ice within a small area. For example, late-winter (April) under-ice storage capacities have been estimated to be as high as 400,000 barrels per km^2 from surveys of fast ice along the Alaskan North Slope (Kovacs et al., 1981). Early winter values have been computed to be about a half as great, reflecting the smoother ice under surface early in the growth season.

As the natural oil containment increases with ice thickness (rougher under surface), the area needed to contain a given spill volume decreases steadily throughout the winter, as shown in Fig. 2-1 below. The average oil layer thickness under the ice can range from several centimeters for spills in early winter to tens of centimeters in April for a spill under ice at the end of the ice growth cycle. The maximum oil thickness in the deepest pools could vary from 10 to over 30 cm, respectively. The implication is that regardless of the time of year, any oil spilled under ice will tend to be naturally contained within a relatively small area when compared to an identical volume spilled on open water.

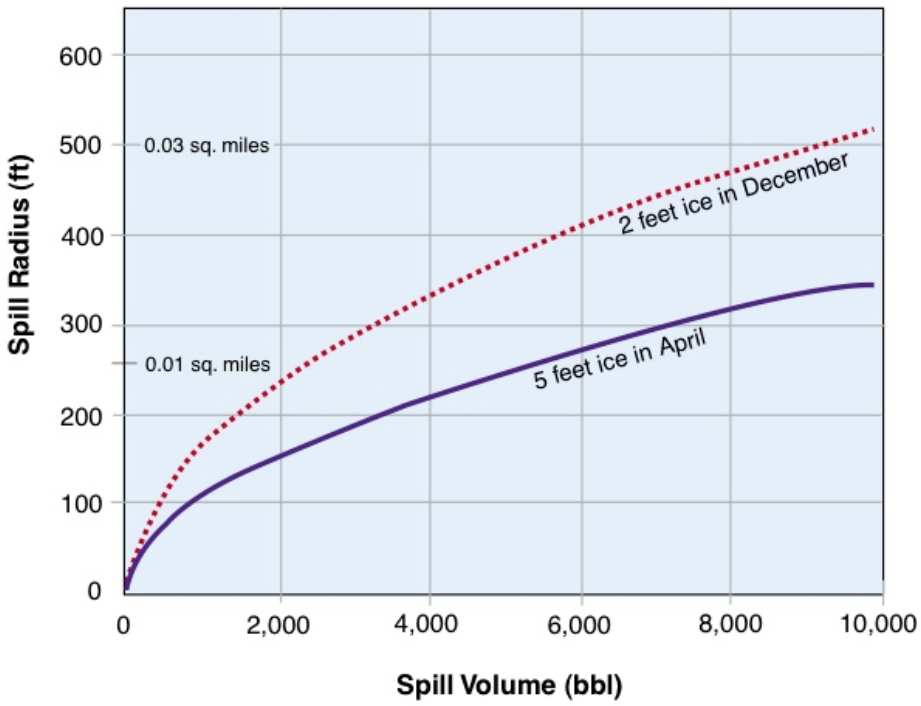

Figure 2-1 Predicted Radii of Spills of a Given Volume Spilled Under Landfast Ice (Dickins and Buist, 1999)

In moving pack ice over a fixed discharge point (e.g. subsurface blowout) the under-ice cavities (natural variations in thickness resulting from the variable insulating effects of an uneven snow cover) are unlikely to be filled beyond a small percentage of their capacity. In that case, the deposited film thickness will be directly proportional to the ice speed. The same "conveyor belt" concept also applies to film thickness on the surface of the ice from an atmospheric release deposited onto moving ice.

Spills under ice during the active solid ice growth period (November to April) will become encapsulated by new ice growth beneath the oil layer. Under Arctic (Beaufort Sea) conditions, this encapsulation process has been observed to occur within 24 to 72 hours, depending on ambient temperatures and growth rates (Norcor, 1975; Dickins et al. 1981). The end result is a trapped oil layer with solid ice above and below the oil is shown in Fig. 2-2.

Figure 2-2 Oil encapsulated in ice during an experimental spill in Alaska. Photo: A. Allen

2.2 Brine Inclusions

An understanding of the process of brine inclusion within a growing sea ice sheet and the subsequent behavior of these brine pockets through the winter has an important bearing on radar performance, in particular the ability for the radar energy to penetrate to certain depth in the ice. In addition, the condition of the brine channels at different stages in the ice growth and melt cycles affect the oil layer characteristics, determining for example whether the oil resides as a discrete trapped layer or as a diffuse boundary with vertical migration through all or part of the ice sheet.

Brine is entrapped within an ice sheet during the freezing process in the form of fine pockets of fluid between platelets of pure ice. The amount of salt trapped in the ice is principally dependent on the rate of freezing. As the ice thickens, the growth rate decreases and brine is expelled more efficiently. At any given temperature, the fluid within the brine channels is always at a salt concentration such that it exists in equilibrium with the surrounding pure ice crystals. The predominant salt in seawater, $NaCl.H_2O$, precipitates out at -22.9°C (Sanderson, 1988). This means that in order for the brine pockets to exist in a primarily crystalline (non fluid) state, the ice temperature needs to be below this value. In most areas outside the High Arctic, air temperatures are such that only the upper ice layer will experience temperatures below this threshold for any length of time. Consequently, most of the entrapped brine will exist in a concentrated fluid state.

The gross brine volume fraction brine volume (V_b) within any sea ice sheet is approximated (Frankenstein and Garner, 1967) by a relatively simple function of temperature and salinity expressed as:

$V_b = 0.001S\ (0.53\text{-}49/T)$

where S is salinity in ppt,
T is temperature in °C

Crude oil spilled underneath a sea ice sheet will immediately penetrate the soft, porous skeletal layer of fragile and separate ice crystals projecting downwards at the freezing interface (See Fig. 2-3). Once this initial saturation process has occurred and the oil spreading has stabilized, the oil will either remain static, or begin to migrate vertically through brine channels. The actual sequence of events in any given spill will depend primarily on the degree of connectivity between individual brine pockets.

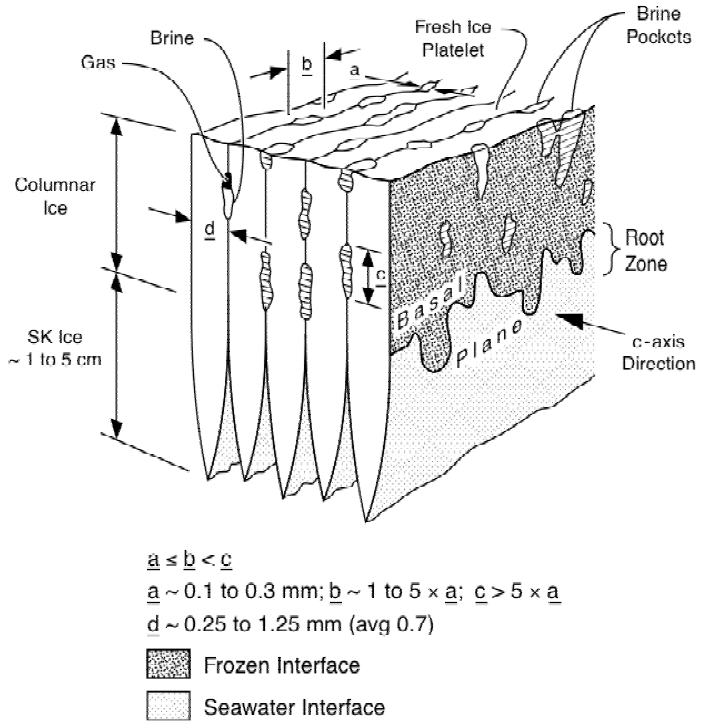

Figure 2-3 Sea ice crystal structure. Source: Kovacs (1996)

In a cold sea ice sheet with a close to linear temperature profile connecting the cold surface (<<0°C) and relatively warm ice water interface (-1.9°C) the brine exists in discontinuous pockets with no clear pathway for the oil to migrate any significant distance. Over the course of the winter ice growth period, brine pockets naturally migrate downwards as a result of the normal winter temperature gradient.

Energetics favor continual melting of the ice at the warmer end of the brine pocket and refreezing at the colder end. As a result, the pocket tends to migrate towards the higher temperatures, becoming larger and longer as they pass into progressively warmer surrounding ice at greater depth (Zubov, 1945). Eventually, the pockets coalesce to form major continuous channels in the order of 0.1 to 10 mm diameter. In the spring, the ice normally experiences a reversal in temperature gradient with both the upper and lower ice surfaces being warmer than the interior (Sanderson, 1988). In this situation, brine is expelled from the sheet in both directions. As a result, the gross salinity (total salt content) of the sheet decreases with time and the brine channels remain to form a continuous pathway from a trapped oil layer to the ice surface. Once the ice reaches this state of deterioration, the rate of oil migration can be extremely rapid. For example, Norman Wells crude oil released under two meters of ice in the Balaena Bay experiment on the Arctic coast reached the ice surface within one hour in late May (Norcor, 1975).

Through this process of migration through brine channels, oil trapped within thick ice during a winter spill (e.g. January to April in Arctic areas such as the Beaufort and Kara Sea or February to March in more southerly areas such as Svalbard and the central Chukchi Sea) will migrate rapidly through the ice in the April to May period and appear on surface melt pools in May and June.

Partial migration of oil has been observed in ice cores extracted throughout the winter, with the vertical rise depending largely on the internal ice temperature (Norcor 1975). Oil will tend to rise to the level in the ice where the temperature is close to 8°C. Depending on the ice thickness at the time of the spill an initial vertical migration of 10 to 20 cm could occur rapidly, with the oil stabilizing at that level until the ice sheet warms further in the spring. This partial migration case is used in this study as one of the model simulation scenarios (See discussion in Chapter 5).

The overall rate of oil migration through the ice sheet is also affected by the depth at which the oil lens trapped within the sheet (small isolated oil particles take longer to surface) the oil viscosity and potentially the ice salinity (less saline ice will have fewer brine channels). Heavier crudes or emulsified oil take longer to rise through the brine channels in the ice, as do small isolated oil particles from a subsurface oil and gas blowout (Dickins and Buist, 1981). SINTEF studied the rate of oil migration from a spill of 3,400 l Stafjord crude spilled under 65 cm of fjord ice off Svea on Svalbard in March 2006 (Dickins et al. 2006). See Fig. 2-4 below. The results compare closely observations from a previous oil-under-ice experiment in the Canadian Beaufort Sea carried out in 1979/80 (Dickins et al., 1981). In that project oil from the first spill rose through a similar ice thickness (60 to 70 cm) to reach 100% exposure in approximately 40 days from first appearance under the snow, very similar in timing to the dates of oil appearance documented on Svalbard (Fig. 2-4).

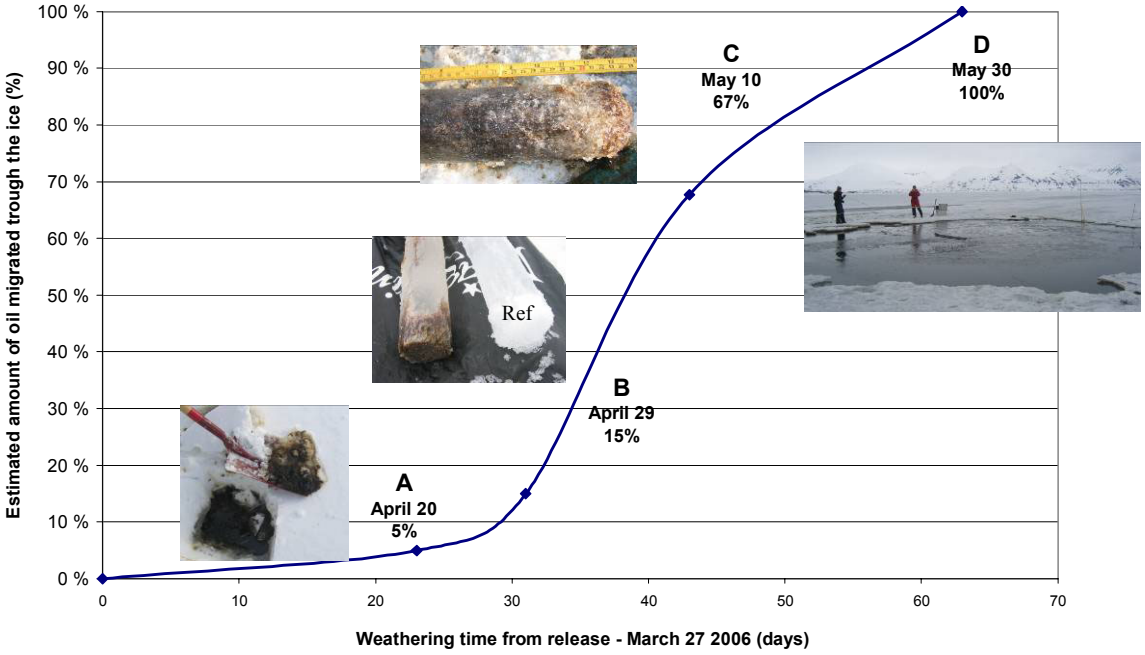

Figure 2-4 Estimated amount of oil penetrated through the brine channels in the ice and available on the ice surface in April/May 2006 on Svalbard. Inserted pictures show oil on top of snow (A), cores drilled through the ice to quantify oil captured in the ice (B + C) and the final melt pool (D). Brandvik and Faksness in Dickins et al. (2006)

2.3 Spreading on Ice and Snow

Oil can be deposited onto the surface of ice from a number of possible sources, for example:

- Surface blowout resulting in a plume of oil droplets falling downwind from a source such as a bottom-founded production structure or artificial island surrounded by stable or moving ice. Oil deposited in this manner will saturate the existing snow layer and then potentially be covered by fresh snow later in the season.
- Surface runoff of oil deposited on the deck of a drilling structure or surface of an artificial island. At some point, the volume of oil may exceed the containment capacity built into the facility. The spill can then run out onto the ice surface and spread under the snow cover.

The spreading of oil on the ice surface is similar to spreading of oil on land or snow. The density and viscosity of the oil controls the rate of spreading and the final contaminated area is dictated largely by the surface roughness of the ice. Oil spilled on ice spreads much more slowly than on water and covers a smaller final area with much thicker equilibrium thickness than on water.

Figure 2-5 shows the result of a diesel spill from a ruptured tank barge frozen in for the winter. The layer of oil-saturated snow is clearly visible as a result of the oil spreading at the ice snow interface.

Figure 2-5 View of oil saturated snow layer on top of the ice following an accidental spill in the Beaufort in 1979. Photo: D. Dickins

Figure 2-6 shows the final estimated area of spills on ice as a function of spill size and ice roughness drawn from some of the earliest experimental spill results documented by McMinn (1972). Smooth first-year sea ice has an average surface roughness in the 0.01 - 0.1 ft. range. Individual ice deformation features such as rafting, rubble and pressure ridges can lead to localized increases in roughness up to tens of meters in elevation above sea level (for example, in the case of extreme grounded ridges along the seaward edge of the fast ice). Any oil spilled on the surface of rough ice may be completely contained in thick pools bounded by ridge sails and ice blocks.

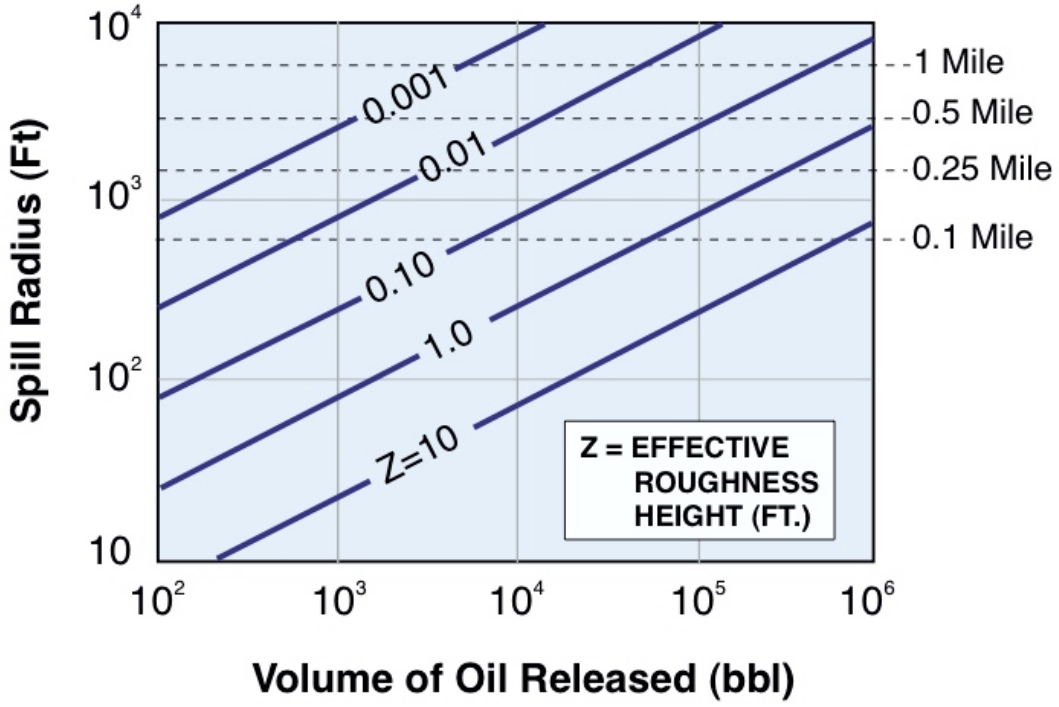

Figure 2-6 Oil spreading on the surface of ice (McMinn, 1972).

The spreading characteristics of oil on snow have been studied earlier by a number of researchers (e.g. Mackay et al. 1974). The state of knowledge in this field is summarized in Owens et al. (2005):

> "Depending on the snow conditions, oil may remain at or near the surface or drain through the snow or into ice cracks. Much of the oil is often hidden from view. The basic principles of snow and ice and oil behavior are relatively well understood. Equations and models are available to estimate rates of infiltration, spreading, migration, or evaporation for oil in snow (Bech and Sveum 1991; SL Ross and DF Dickins 1988). However, there is limited understanding of the actual mechanics of oil behavior or transport pathways in snow. For example limited knowledge exists regarding how oil migrates through a non-uniform snow cover. As a consequence, it is difficult to estimate where the oil might accumulate, a critical question for responders. The few observations published from spills or field experiments indicate that oil transport and migration mechanisms are likely to be complex, particularly if the structure of the snow is not uniform or contains ice layers (a common occurrence in areas with frequent freeze/thaw cycles)."

2.4 GPR Oil in Ice Detection Capabilities

The scope of oil-in-ice detection research supported by MMS over the past four years is outlined in Chapter 1.0. As a result of these studies, the scientific team was able to begin the current project with basic set of conclusions and assumptions regarding the expected future potential of GPR in a number of specific situations.

Ground Penetrating Radar was successfully deployed from the ice surface in both tank tests and a field environment to detect and map the presence of oil under up to 65 cm of ice. In 2006, the relatively warm (high brine volume) ice represented close to a worst case in terms being able to penetrate the ice with sufficient signal strength to profile the ice/oil/water interfaces. In summary, even under unfavorable spring-like ice conditions, the radar field results demonstrated that a well-defined, measurable anomaly is induced by the presence of oil films as thin as 1-3 cm under the ice. The surface radar imaging attributes provided a strong indicator where oil is present and could be clearly differentiated from the background response (areas with no oil).

Airborne radar shows strong potential to detect oil at the snow/ice interface with existing systems, and to measure ice thickness and detect oil at the ice/water interface with higher-powered systems and/or colder ice in the near future.

It is expensive and logistically difficult to conduct more than a handful of large-scale field experiments. Consequently, this project was designed around the approach of intensive computer modeling to understand the radar response to a variety of sea ice conditions and oil types and distributions, and to fully define the limitations of the radar method far beyond what can be achieved in limited field-testing.

All of the experiments to date have been performed on first-year ice with relatively even top and bottom surfaces. Detection of oil under ice through multi-year ice or rafted/ridged first-year ice is expected to be extremely difficult if not impossible. While snow cover does not substantially affect radar penetration, the presence of voids and upturned blocks within rough ice would present a major challenge to radar profiling. The focus of all the work to date (and the current study) is on relatively smooth, solid ice sheets without extensive voids or discontinuities. This type of ice is characteristic of much of the nearshore region of the Beaufort Sea (out to approximately 12 m water depth) as well as much of the offshore region (beyond 30 m water) in mid-winter.

The state of knowledge surrounding GPR capabilities for oil-in-ice detection is summarized below from findings of MMS-sponsored research since 2004:

- Surface-based ground-penetrating radar (GPR) operating at 500 MHz clearly delineates changes at the ice water interface caused by emplacement of oil. GPR operated from the ice surface is capable of differentiating oiled regions of the ice under surface from the background response.

- Based on a qualitative comparison of the measured oil thickness distribution and radar results, it appears that the lower detection limit at a frequency 500 MHz is on the order of 1 to 3 cm oil film thickness, agreeing with findings from the 2004 tank tests at CRREL.

- The existing, portable commercial GPR systems are capable of profiling natural sea ice sheets as thick as 2 m as late as April (warmer ice later in the ice season could reduce the allowable thickness).

- The airborne radar tests in 2006 were not as definitive as the surface surveys, however it appeared that the 500 MHz system was capable of penetrating at least 0.65 m of relatively warm sea ice representing a worse-case for radar operations. The potential to detect oil from an airborne platform in the future looks promising based on results from the initial Svea trials. At a frequency of 1000 MHz, it was possible to image the snow pack and snow ice interface in detail from low altitude (5 to 10 m), suggesting a strong potential to detect oil at the ice/snow interface with existing off-the-shelf systems.

- Apart from the basic parameter of the strength of the reflected signal, there are a number of different reflection properties (commonly referred to as attributes) that show greater sensitivity to varying thickness of oil films. For example, a phase change (or change in the reflected wave shape) was observed after oil was placed under the ice and this may prove to be the most robust indicator of the presence of oil. The phase change was most prevalent in the area of thick oil where reversed polarity was observed. A high amplitude response was also observed in areas where the oil film thinned and reflections from the top and base of the ice interfere. Optimal detection in an uncontrolled setting (without the benefit of knowing ahead of time where the oil lies within a general area) will require simultaneous computation and analysis of each of these waveform attributes. Software developed under an earlier phase of this project is designed with this capability (Bradford, 2005).

- While GPR technology appears full capable of determining whether oil is present or not, it is considered unlikely that meaningful measurements of film thickness can be made under typical field conditions. This is largely due to a combination of the lateral heterogeneity of ice at the surface and within the ice sheet itself, and the natural complexity inherent in the crystal structure at the growing ice/water interface (see Fig. 2-3 above). These complexities have a significant impact on the GPR attributes needed to resolve differences in oil film thickness.

3. Overall Program Scope and Objectives

The scope of the current study developed as an outgrowth of recommendations following the 2006 Svalbard trials (Dickins et al. 2006). That report recommended:

1. Modeling the expected radar response to different oil in ice scenarios. Parameters should include (not limited to): ice thickness, salinity, and temperature; and oil film thickness. Since radar is sensitive to electric polarizability, radar performance is not directly linked to oil specific gravity however there may be an indirect link since longer chain hydrocarbons tend to be more polar.
2. Evaluating the potential to develop operational airborne radar system capable of detecting oil under ice of different composition and thickness (related to parameters defined above).
3. Continuing to improve the display interface to reduce the level of training necessary for responders to use GPR in a field setting (an initial stage of interface development was achieved in an earlier Phase of work sponsored by MMS in 2005).

The current study was designed around the following main tasks:

- Review available systems and potential sources of necessary hardware that could provide a basis for future higher-powered airborne systems (if this proves necessary) to achieve successful detection from a helicopter platform. The key issue is being able to combine in a single system the conflicting requirements of needing a relatively high frequency to resolve thin oil films while achieving penetration of a relatively conductive material such as sea ice (accomplished most effectively at lower frequencies).
- Assess the timelines and level of funding required to develop a prototype airborne system with sufficient power to map the ice/water interface from a helicopter at 5 to 15 m altitude.
- Use existing Boise State GPR modeling software to carry out computer simulations, establishing a library of expected signal characteristics for a variety of potential oil under-ice and oil trapped-in-ice scenarios. Ice properties and oil-in-ice configurations will draw on experience with previous large-scale experimental spills (Norcor 1975; Dickins and Buist 1981) and GPR trials in 2004, 2005 and 2006 summarized in Chapter 1. Model outputs will be verified by simulating conditions at the Svalbard 2006 field trial and 2004 CRREL basin experiment, and comparing results.
- Assess the future potential of off-the-shelf systems to map oil on top of solid ice, buried under varying thicknesses of snow. This aspect of the program will build on the high-resolution surface profiles obtained on Svalbard in 2006 (with no oil on the surface).

Findings from each of these tasks are summarized in the following chapters.

4. Hardware Evaluation

There are many commercial airborne radar systems, however most are designed either for range finding (altimetry), defense applications such as target identification, or meteorological applications. We have found no commercial airborne radar system designed specifically for subsurface imaging. This is not to say that such studies have not been done, in fact there are many examples of airborne radar deployment for subsurface imaging. However, these studies have been conducted using radar systems designed for ground deployment similar to the systems we have deployed in both ground based, and airborne modes in earlier phases of this study.

Although there are no commercially available solutions, there are two research groups that have been developing airborne radar systems over the last 15-20 years, primarily for glacial ice-sheet imaging. Their programs are summarized below.

- *University of Texas* - Most of the research for airborne radar systems has been focused on ice mapping in Antarctica where a radar system is installed in a Twin Otter plane and flown over the ice. The radar system has a frequency range of 52.6-67.5 MHz, far too low for resolving oil films. More information can be found at http://www.ig.utexas.edu/research/projects/soar

- *The Center for Remote Sensing of Ice Sheets (CReSIS)* at the University of Kansas – The Radar Systems and Remote Sensing Laboratory is developing airborne radar to map the internal layers in shallow and deep ice to determine the presence/absence of water between ice and bedrock. The operational ice sheet imaging radar operates at 150 MHz but the same team has recently built a prototype airborne radar system for sea ice profiling that operates in the 400 MHz range. This system is undergoing continued testing and development but could be a suitable solution for the oil under ice problem. More information can be found at https://www.cresis.ku.edu/

Clearly the CReSIS[JHB1] team has the most relevant system for the oil in ice application. We have discussed the potential for future collaboration with Dr. Prasad Gogineni who is heading the sea ice radar development group. This collaboration may include participation in the Joint Industry Arctic Oil Spill Research Program and side-by-side comparison of the CReSIS system with our commercial GPR system deployed in airborne mode.

The CGISS group at Boise State University is in the process of expanding their expertise to include radar hardware solutions by taking on an experienced new staff member. Future development of improved airborne systems could utilize the modeling results of this study to improve performance and expand the window of opportunity with respect to ice conditions and allowable flight envelopes (speed and elevation).

5. Scenario Development and Scope

The modeling effort (see results in Chapter 6) utilizes a set of scenarios that describe a range of ice, oil and snow configurations expected from a variety of spill sources.

In order to select a realistic number of credible scenarios it was necessary to review the potential range of spills from both exploration and production activities that could result in oil under ice, encapsulated within the ice sheet or on the ice surface capped with snow.

The following matrix shows a range of spill types vs. water depth for exploration and production activities, focusing on the Beaufort region. The matrix is also applicable in large part to the Chukchi Sea area except that gravel exploration and or production islands are not likely in this area given the steep bottom slopes and unpredictable nature of the fast ice zone south of Point Barrow.

Table 5-1

Spill Source and Possible Oil-in-ice Configurations vs. Water Depth					
Spill Source	**Water depth (m)**	**Oil on Ice**	**Oil Under Ice**	**Trapped Layer**	**Comments**
Exploration					
Subsea blowout	2 to 20	N/A	N/A	N/A	Too shallow for floating drilling rigs
Subsea blowout	30 to 200	N/A	Possible	Possible	Most likely to see oil under thin ice late Oct/Nov
Surface blowout	2 to 15	Possible	N/A	N/A	Fallout from surface oil plume, saturated snow around gravel islands and/or oil running off the island and onto the surrounding ice
Production					
Subsea blowout	Any depth	N/A	N/A	N/A	Floating rigs (source of subsea blowouts) not likely for year-round production in ice
Surface blowout	Any depth	Possible	N/A	N/A	Fallout from surface plume
Pipeline leak/rupture	Any depth	N/A	Possible	Possible	No detection possible in shear zone areas with highly deformed ice

The final suite of scenarios were selected to satisfy the following general criteria:

- Sufficient permutations and combinations of oil, ice and snow conditions and properties to allow predictions of radar performance over a wide range of realistic spill situations (see ice inputs summarized below in 5.1).
- Demonstrated link to ongoing and projected exploration and production development activity on the Alaskan OCS in the Chukchi and/or Beaufort Sea regions (see preceding matrix).
- Practicality in terms of not trying to achieve the "impossible". For example detecting oil trapped under 60 feet of grounded pressure ridges and rubble in the shear zone.

The scenarios incorporate variations on three basic oil and ice configurations:

1. Oil under the ice
2. Oil trapped as a layer within the ice sheet
3. Oil on the ice surface under snow

5.1 Oil and Ice Scenario Inputs

The baseline ice conditions (thickness, temperature and salinity), expected oil layer thickness and timing of migration were based on historical field measurements from various studies e.g. Norcor (1975), Dickins and Buist (1981). Figure 5-1 and Tables 5-2 and 5-3 summarize the model input values following the natural ice growth cycle from October to June, representative of the Alaskan Beaufort Sea.

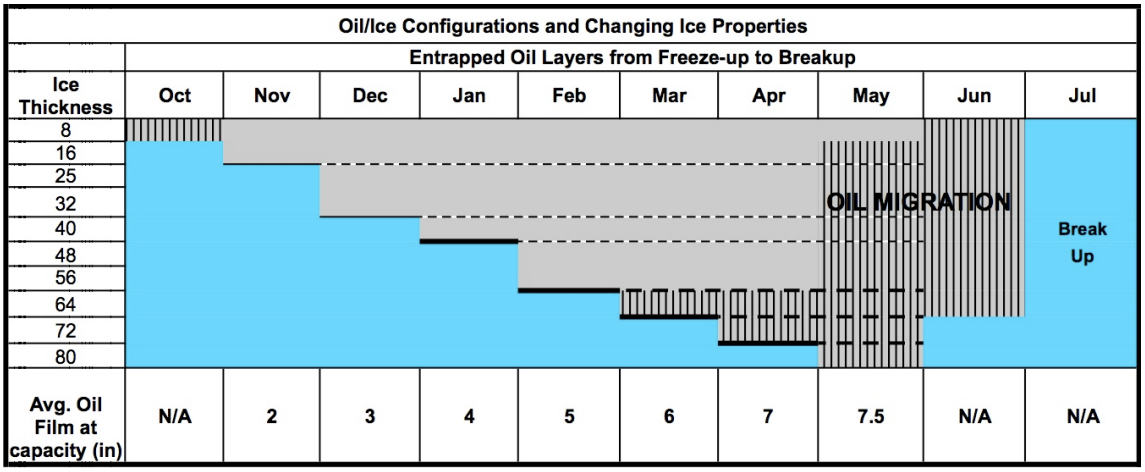

Figure 5-1 Oil-in-ice configurations throughout a typical first-year ice cycle in the Beaufort Sea, from freeze-up to break-up. Ice thickness in inches.

Tables 5-2 and 5-3 show the ranges of ice temperature and salinity used as input into the Scenario 3 scenario models based on a typical Beaufort Sea environment. Brine volumes were calculated from this data as a primary input into the modeling process using the expression developed by Frankenstein and Garner (1967).

Table 5-2
Representative Ice Salinity Profiles Varying by Month
(from historical Field Data)

	Oct	Nov	Dec	Jan	Feb	Mar	Apr	May	Jun
Depth (in)	Internal Ice Salinity ppt								
2	15	12	12	12	10	8	5	1	1
8	9.7	6	6	5.5	5	3.5	4.3	3	1.8
16	34	5	5.5	5	4.7	5	5	2	2
25	34	7	5.7	4.8	4.5	3.7	4.6	3	2.5
32	34	34	6	5	4.5	4.1	4.6	3	2.7
40	34	34	34	5.5	5.2	4.1	4	4	3
48	34	34	34	34	5	4.5	3.7	4	3
56	34	34	34	34	34	5	3.7	4	3
64	34	34	34	34	34	6	3.5	4.5	3
72	34	34	34	34	34	34	5	5	15
80	34	34	34	34	34	34	15	15	15
Bulk Salinity	**9.5**	**7**	**6**	**5.5**	**5.2**	**5.1**	**5**	**5**	

Table 5-3
Representative Internal Ice Temperature Profiles Varying by Month

	Oct	Nov	Dec	Jan	Feb	Mar	Apr	May	Jun
Depth in)	Temperature								
AIR	-7	-13	-25	-25	-29	-30	-6	-3	3
2	-5	-7	-12	-17	-18	-19	-8.5	-3	-0.5
8	-3	-5	-10	-16	-17	-17	-8	-2	-0.8
16	-1.8	-4	-7	-13	-15	-14	-7.5	-2.5	-1
25	-1.8	-2.3	-3	-11	-12	-11	-6.5	-3	-1.5
32	-1.8	-1.8	-2.3	-7	-9	-8	-5.5	-3	-1.7
40	-1.8	-1.8	-1.8	-3	-6	-6	-4	-2.5	-1.5
48	-1.8	-1.8	-1.8	-1.8	-4	-4	-3.5	-2.2	-1
56	-1.8	-1.8	-1.8	-1.8	-1.8	-2	-3	-2	-0.5
64	-1.8	-1.8	-1.8	-1.8	-1.8	-2	-2	-2	-0.5
72	-1.8	-1.8	-1.8	-1.8	-1.8	-1.8	-2	-2	-0.5
80	-1.8	-1.8	-1.8	-1.8	-1.8	-1.8	-1.7	-1.6	-0.5

5.2 Primary Scenarios

Table 5-4 outlines the scope of each scenario utilized in the modeling phase of study in terms of oil placement in the ice and ranges of parameters covered in the modeling (snow depth, oil layer thickness, ice thickness, salinity, temperature etc.). Scenarios are shown as graphic representations in the discussion of modeling methods and results in Chapter 6 (following).

Table 5-4
Summary of Oil in Ice Scenarios

Scenario #	Title	Parameters	Range
Oil on Ice			
1	Wedge Model	Saturated snow depth	1 to 5 cm
		Clean snow depth	Max of --- and tapering to zero
2	Case Study after Mackay et al. (1974)	Variable oil penetration from actual trials	Random pockets
Oil Under and Trapped within Ice			
3	***1-Dimensional reflectivity modeling***		
3a		Time of year	Nov to April
		Ice thickness (h)	50 to 200 cm
		Ice temp and salinity	varying vertical profiles with time
		Oil thickness	20% of (h)
		Oil location	Under ice
		Ice/water interface	Smooth
3b	as 3a but with trapped layer within the sheet	Oil thickness	increasing with depth (time of spill)
3c	as 3b but with increase in salinity above the oil layer	Oil layer	1 cm
3d	as 3a but with snow	Time of year	Feb only
		Snow depth	10 to 20 cm
		Ice temp profile	Variable
		Ice salinity	as per 3a - Feb
4	***2-D Finite Difference - Constant sinusoidal ice/water boundary***		
	Note: #4 run with and without oil under the ice	Time of year	Feb
		Ice/water interface	Sinusoidal
		Amplitude of under ice variations	20 cm peak to trough
		Wavelength of under ice variations	5 m
		Oil thickness	0 to 20 cm
4a	as 4 but with partial oil migration from ice base	Vertical migration	random up to 12 cm above the ice base
4b	as 4a but with partial migration from a trapped oil layer	Trapped oil layer	2 cm thickness at 60 cm depth
5	***Decaying sinusoidal ice/water boundary***		
	Note: #5 run with and without oil under the ice	Maximum amplitude of under ice variation	20 cm
		Wavelength of under ice variability	5 m decaying to 0.5 m in 12 m dist.
		Radar elevations	0, 15, 30 m
6	**Slow Leak from Marine Pipeline under Solid Ice**		

5.3 Second Tier Scenarios

In addition to the scenarios selected as the basis for modeling GPR performance (summarized above in Table 5-4), the project team identified a number of other interesting scenarios. While viewed as a lower priority in terms of their likelihood of occurrence and or geographic relevance to marine areas regulated by MMS, one of more of these situations could be further developed and modeled in follow-on phases. These so-called *Second Tier Scenarios* are outlined as follows:

- Oil with Gas: Subsea blowout under ice thick enough to contain large volumes of gas accumulating in thinner ice areas and relatively thin oil films. This would involve modeling an ice/gas/oil/water interface combination as illustrated in Norcor (1977).

- Multiyear ice: With recent documented shifts in the age distribution of the pack ice within the Arctic basin (e.g Rigor and Wallace 2005), the probability of significant concentrations of multi-year ice being associated with an exploration spill scenario is significantly lower than during the last period of intensive exploration offshore Alaska in the 1980's. Based on ice conditions in the past decade, substantial concentrations (over 30% coverage) of old ice can now be expected no more than 2 years in ten in Beaufort Sea nearshore region (vicinity of 30 m water depth). This scenario could build on results obtained from the only field spill involving oil under multi-year ice (Comfort et al., 1983). The much lower salinity of old ice compared to first-year ice could enable GPR profiling of significantly thicker sheets (beyond 2 m). Model simulations could help determine the realistic upper limit.

- 2D Snow Depth: Vary snow depths in the 2D model. This would produce varying temperature profiles within the ice sheet over relatively short horizontal dimensions (tens of meters) and more closely mimic natural conditions.

- Bottomfast Ice Spill: Oil pool trapped at the ice/seabed interface in the bottomfast ice zone. This scenario also involves a chronic leak or rupture from a buried marine pipeline but in shallow water (less than 2 m depth) where the fast ice rests on the seabed of vast areas of the Beaufort Sea nearshore region. This scenario would generally apply to State waters off the Alaskan North Slope (potential for joint funding between MMS and ADEC).

- Warm oil spilled onto snow: This scenario would apply mostly to the case of on-land spills to frozen ground from pipeline ruptures or leaks (live crude).

6. Computer Modeling

The six primary scenarios defined in Chapter 5 were utilized as a basis to evaluate the capabilities of GPR in detecting oil in a variety of situations at different times of year and with varying ice and snow properties.

6.1 Introduction to Basic Radar Theory and Nomenclature

Ground Penetrating Radar (GPR) has been used in numerous arctic studies to image both internal structures within snow (e.g., Bradford and Harper, 2003), the ice/water contact and subsurface geology below freshwater ice (Best et al., 2005; Bradford et al. 2005; Brosten et al., 2006), and the sea ice/sea water contact (Nyland, 2004; Kovacs, 1977). In GPR studies, a transmitting antenna generates a downward-directed oscillating electric field that propagates through the subsurface and is reflected back toward a receiving antenna at boundaries separating materials with differing electric properties (dielectric constant, electric permittivity, and conductivity). The reflected wave field is recorded and used to produce a reflector map in travel time, usually reported in nanoseconds (ns) or microseconds (μs). This reflector map, similar to a cross section of the subsurface, is an indicator of electric property contrasts which usually, but not always, occur at material boundaries. Often, a reflection may be interpreted in travel time (e.g. the reflection occurs at xx ns). This merely reflects the amount of time that it takes for the GRP signal to travel from the surface to the reflector and back again. With knowledge of the radar velocity (or dielectric permittivity) it is possible to calculate the depth to the reflector if the travel time is known.

The large permittivity contrast between sea ice and sea water (~5:88) and between sea ice and oil (~5:2.2) suggests we can derive an accurate map of subsurface boundaries in these conditions using very high frequency GPR antennas (~500 MHz - 1 GHz), and successful results from the two field projects conducted during earlier phases of this project (Dickins et al, 2005; Dickins et al, 2006) support this conclusion.

The resolving power of the GPR system limits the thickness of sub ice oil that can be measured directly, i.e. by measuring the travel time difference between wavelets reflected from the top and bottom of a layer. The wavelength of the signal controls the resolution, with a shorter wavelength signal capable of resolving finer features. When a layer is thinner than about ¼ of the dominate wavelength of the GPR signal, it is impossible to clearly differentiate wavelets reflected from the top and bottom of the layer and a simple reflector map is not sufficient to confidently identify the presence of oil under the ice. In this case, rather than relying on a direct measure of travel time differences, detailed measurements of the waveform are used to detect the presence of thin layers and characterize their properties. In the geophysical literature, this type of analysis is commonly referred to as attribute analysis. The most commonly used group of attributes are calculated from the analytic trace (a complex form of the radar trace) and are termed instantaneous attributes.

These include measures of the shape (instantaneous phase), the spectrum (instantaneous frequency) and the reflection strength (instantaneous amplitude). Attribute analysis is commonly used in oil and gas exploration to identify reservoirs of hydrocarbon in sedimentary rocks (Chopra and Marfurt, 2005). Amplitude and phase measurements can be made from typical fixed antenna GPR data, which is relatively fast and inexpensive to acquire. A number of studies have shown that attribute analysis of GPR data can be effective for identifying contaminants in sedimentary groundwater systems (Orlando, 2002; Bradford and Wu, 2007; Bradford and Deeds, 2006; Bradford, 2007). Similar methods for detecting oil spills under sea ice were first proposed by Goodman et al. (1985), and our previous field work has verified the capability to detect oil under sea ice in lab (Dickins et al, 2005; Bradford et al., 2005) and field conditions (Dickins et al., 2006).

Water strongly attenuates the radar signal, with the rate of attenuation increasing as the dissolved solid concentration (electric conductivity) increases. Thus, brine contained within pockets or channels in ice may limit signal penetration. When sea ice forms, predominant ocean currents cause preferred alignment of the c-axis of the ice crystals. This in turn results in a preferred alignment in the distribution of brine within the ice matrix. Radar attenuation depends strongly on the brine volume and orientation and the ordered distribution of brine channels produces a directional dependence, or anisotropy, in the radar attenuation. This occurs because the radar signal is polarized. The antennas used in this study are linear dipole antennas. When the antenna is parallel to the c-axis of the ice, the electric field polarization is also parallel to the c-axis and the signal undergoes maximum attenuation. Conversely, when the antenna is perpendicular to the c-axis, the signal undergoes the minimum attenuation. This effect can also be considered in terms of electric conductivity – maximum conductivity occurs along the direction parallel to the c-axis. It is important to recognize that entrapped brine and sea ice anisotropy may alter the measured GPR attributes and that these characteristics may not easily be quantified in field data. This problem is minimized in field data analysis by computing attributes relative to a background response that is measured from the data.

The objective of this project is to predict the radar response to a variety of scenarios with oil under, in, and on sea ice and snow. This objective is met through numerical modeling algorithms. First, it is important to recognize that the GPR signal is sensitive to the electrical properties of the ice. Therefore, the initial step in running the numerical model is to estimate the electrical properties of the ice from parameters that would likely be measured in the field, specifically from ice temperature and salinity. Ice temperature and salinity both play a strong role in determining the brine volume, which in turn is the primary parameter controlling GPR signal penetration.

After the electric property model is determined, the GPR response is modeled by solving Maxwell's equations. Maxwell's equations are a set of four coupled differential equations that govern electromagnetic fields and for purposes of this study, the solution of these equations simulates the propagation of a radar signal through the media of interest.

For models that contain smooth lateral variations, we can use the reflectivity method to simulate GPR wave propagation. The reflectivity method assumes that there are only vertical variations in the subsurface and involves solving a recursive formula that is derived from an energy balance at all interfaces in the model. The method produces an exact analytical solution to Maxwell's equations for one-dimensional media.

The second method that is utilized is a two-dimensional finite-difference time-domain (FDTD) algorithm that is a commonly used approach for solving partial differential equations. To apply the FDTD method, the model space is discretized on to a fine grid and the differential equations are solved directly. The finite difference method is capable of simulating GPR wave propagation in laterally heterogeneous medium. Drawbacks to the finite difference method are that it is computationally expensive and since it is a numerical approximation the solution is not exact. The accuracy of the solution is improved by decreasing the grid spacing, but this comes at increased computational cost.

6.2 Methods

Boise State University developed a set of numerical modeling tools specifically to study the oil in and under snow and ice problem based on the primary scenarios defined in Chapter 5. These tools include a computation of electrical properties from input temperature and salinity profiles (see Tables 5-2 and 5-3 above) and two different electromagnetic wave propagator codes. These algorithms are described in greater detail below followed by a summary of modeling results each scenario.

6.2.1 Modeling Algorithms

Electric property model: The radar response is controlled by the electrical properties of the medium through which the electromagnetic wave is propagating. These properties include the electric permittivity and electric conductivity of the material. Sea ice is a complex mixture of brine and ice crystals as described under State of Knowledge (See Section 2.2). In natural sea ice the crystals are often aligned with the predominant current leading to azimuthal anisotropy in the electrical properties. Further, the electrical properties depend on temperature and salinity. Because of this complexity, it is necessary to use a set of empirical relationships to derive the electrical properties. For this study an electric property algorithm was employed based on the relationships given by Morey et al (1984). The algorithm proceeds as follows:

1) Input the measured temperature (T) and bulk salinity profile (S)
2) Compute brine volume (V_b) as a function of T and S
3) Compute the brine salinity (S_b) as a function of T
4) Compute the brine conductivity (σ_b) as a function of S_b and T
5) Compute the complex dielectric permittivity of the brine ε_b at the dominant radar frequency (500 MHz for oil in and under ice scenarios, 1000 MHz for oil in and under snow scenarios) as a function of T and σ_b

6) Compute the bulk electric conductivity using Archies law as a function of V_b and σ_b and imaginary component of ε_b, then output to wave propagator. Simulation of the electric field polarized either parallel or perpendicular to the ice crystal alignment is accomplished through choice of the Archie's law exponent (1.5 for parallel or 1.75 for perpendicular polarization). For this study, the perpendicular field was modeled for all simulations.
7) Compute the bulk dielectric permittivity as a function of V_b , the real component of ε_b and the permittivity of crystalline ice, output to wave propagator.

Using this algorithm combined with a library of field measurements of Temperature and Salinity profiles (see Section 5.1) enabled a realistic simulation of natural sea ice conditions and variability.

Wave Propagator 1: Reflectivity Method

The majority of the modeling was conducted with a reflectivity algorithm. The reflectivity method is an exact analytical solution to the electromagnetic wave equation and the code used in this study is similar to that discussed by Cardimona (2002). The radar response is computed in a layered model using a recursion formula that correctly simulates primary and multiple reflections. The computation is carried out in the frequency domain and frequency dependent wave propagation is accurately simulated which is critical for this study where the conductivity values approach the propagation/dispersion limit in many cases. The properties of each layer are constant but smoothly varying material properties are incorporated into the model by dividing the model into many thin layers. The thin layers must be well below the scattering limit (~1/10 – 1/30 of a wavelength) for the radar wavelet being modeled. In all cases below, the ice was divided into 5 mm layers with electric properties interpolated from the vertical electric property distributions described above. The source wave for the code is a plane wave at normal incidence. All simulations were carried out with the source at a height of 1 m above the ice. Therefore all ice-related losses are correctly predicted including scattering losses at the ice/air interface. The predicted response for alternate antenna heights is then simply a function of the distance above the ice, which alters the predicted amplitude according to wave spreading losses in the air. Since our reference height is 1 m, this gives the predicted amplitude for antenna heights greater than 1 m as $A=A_1/h$, where h is the height above the ice and A_1 is the predicted amplitude at an acquisition height of 1 m. This then provides a basis for specifying radar power and signal to noise increase requirements, relative to ground-based measurements, for an airborne deployed radar system.

The advantages of the reflectivity code are that it is computationally efficient and produces the exact radar response. The disadvantage of the method is that it is not capable of modeling the response to sharp lateral heterogeneity.

Wave Propagator 2: Finite-Difference Simulator

To predict radar response to laterally heterogeneous ice/snow models, a numerical model wave propagator was employed which utilizes a finite difference solution to the electromagnetic wave equation. To efficiently simulate acquisition of relative long radar profiles, the source wave for the propagator is a plane wave placed 1 m above the surface. This approach correctly simulates acquisition of a full profile of closely spaced radar traces with common transmitter/receiver positions and eliminates the need to simulate individual source points. Electric property distributions were constructed by first specifying 2D distributions of temperature and salinity, then using the approach described above to calculate the 2D electric property distributions. These distributions were then interpolated onto the finite difference grid. The disadvantage of the finite difference simulator is that it is computationally expensive and is only practical to run for a limited number of scenarios.

Initial Data Analysis

To gauge the potential to detect oil for all scenarios described below, attributes were computed from simulated data following data analysis strategies that have proven successful in field studies conducted for previous phases of this project (See summaries in Chapter 1). These strategies consist primarily of the computation of the instantaneous attributes along the ice/oil/water interface, which include reflection strength, instantaneous frequency and instantaneous phase.

Results obtained by applying these modeling tools and algorithms to specific scenarios are presented in the following section (6.3).

6.3 Scenario Specific Results

The following sections provide a summary of the modeling results for each scenario consisting of:

- A graphic presentation of the scenarios showing the spatial distribution of oil layers and depiction of the different interfaces (air/snow, snow/ice, ice/oil and oil/seawater).
- Specific considerations involved in applying the different modeling tools to each scenario, and:
- A summary of GPR capabilities in each scenario based on the model outputs.

6.3.1 Snow and Oil Configurations

Scenario #1: Wedge model of oil saturated snow (smooth boundaries)

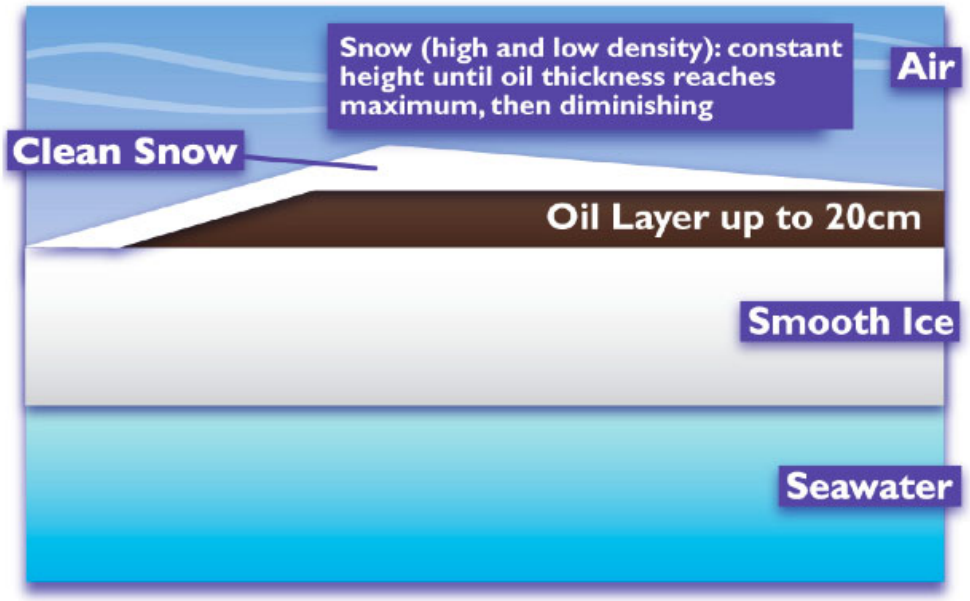

Figure 6-1 Scenario 1

Considerations

For this scenario, the reflectivity model was used to simulate the response to a property model as seen in the schematic diagram. The first step was to calculate the electrical properties for each material in the model. For air, snow, oil and water we used standard published values. Due to the variability in snow density, which affects the permittivity and conductivity, we looked at two cases: one for very high-density snow ($\varepsilon_{snow} = 2.5$, density = 0.66 g/cc) and therefore a permittivity near oil, and one for lower density snow ($\varepsilon_{snow} = 1.5$, density = 0.26 g/cc).

One factor that could enhance the detection of oil under snow is the natural tendency for layer of brine to accumulate at the snow/ice interface. On natural sea ice, brine will be wicked into the looser levels of the snow pack resulting in an increase in electrical conductivity and permittivity close to the snow/ice interface. If oil is introduced at this interface early in the ice growth season, it will block this wicking action, thereby enhancing the anomaly related to the change in electric properties. In that case, the modeled response from this analysis can be considered very conservative (small) compared to the anomaly that would likely be observed for actual field spills onto thin ice before the winter snow cover has had a chance to accumulate.

Results

For the normal condition with lower snow densities, signal anomalies could be detected with oil layers as thin as 1 cm, but for the extreme case of $\varepsilon_{snow} = 2.5$, only a weak response was generated. Such a high density is unusual and was used here to represent the upper bound of possible conditions.

Validation

In cooperation with SINTEF and within the framework of the Joint Industry Program on Oil Spill Response for Arctic and Ice-covered Waters, a controlled field spill was conducted at the field research facility near Svea, on Svalbard. The primary objective of this test was to test the ability of GPR, deployed from a helicopter, to detect a crude oil spill on the sea ice surface but buried by snow. The preliminary results from this test completed in early April 2008 are summarized here.

The experimental site was prepared by constructing two ~4.5 m x 4.5 m test cells on the ice surface; the cells were identically constructed by clearing the snow, then scraping and smoothing the ice surface. The latter was necessary to ensure that the oil would spread uniformly over the test cell. The snow surrounding the cell was very dense (wind packed) and provided adequate containment of the oil without any artificial barriers. One cell served as the experiment control with no oil. In the oiled cell, 400 l of Stratfjord crude were first warmed to room temperature in an indoor facility then poured onto the ice surface (Figure 6-2). The oil flowed smoothly and formed a relatively uniform layer that was approximately 2-3 cm thick. An ~ 1.5 m^2 area remained free of oil in one corner of the cell because of minor variation in ice topography.

Figure 6-2 Sintef personnel pouring oil into the spill containment area for the oil under snow GPR field experiment in April 2008.

Air temperatures during the spill and data acquisition were less than -13C. At these temperatures, the oil rapidly became quite viscous and immobile, preventing further migration outside of the test cell. To prevent accidental contact of wildlife with the oil, a trip wire system with flares was installed around the perimeter of the spill. High winds on the day of the spill resulted in natural wind blown snow cover, 5 – 10 cm thick over the spill and 5 – 20 cm thick over the control cell. This natural snow cover was deemed preferable to artificially covering the spill with shoveled snow as it produced a more realistic spill simulation.

For airborne measurements, the radar system was suspended from the helicopters cargo hook as seen in Figure 6-3 taken during the 2006 oil under ice experiment.

Figure 6-3 Photograph showing the 1000 MHz shielded antennas suspended from the cargo hook of the helicopter.

Data were acquired with the 1000 MHz antennas at altitudes of 5,10,15,20, and 30 m and speeds of 5, 10, 15, and 20 N. Prior to data analysis, the dielectric permittivity of the crude oil ($\varepsilon_{ro} = 3.5$), wind blown snow cover ($\varepsilon_{rs} = 1.4$), and sea ice ($\varepsilon_{ri} = 4.5$) were measured using radar traveltime methods. These measurements were then used to predict the radar response. With this set of parameters and oil thickness varying from 2 – 3 cm it was expected that a significant reduction in reflected radar amplitude would be observed in the oiled cell relative to the control cell, and this was the response that we observed in the field data. Figure 6-4 shows this effect for data acquired at an altitude of 5 m and speed of 5kt. The presence of the oil is easily detected qualitatively.

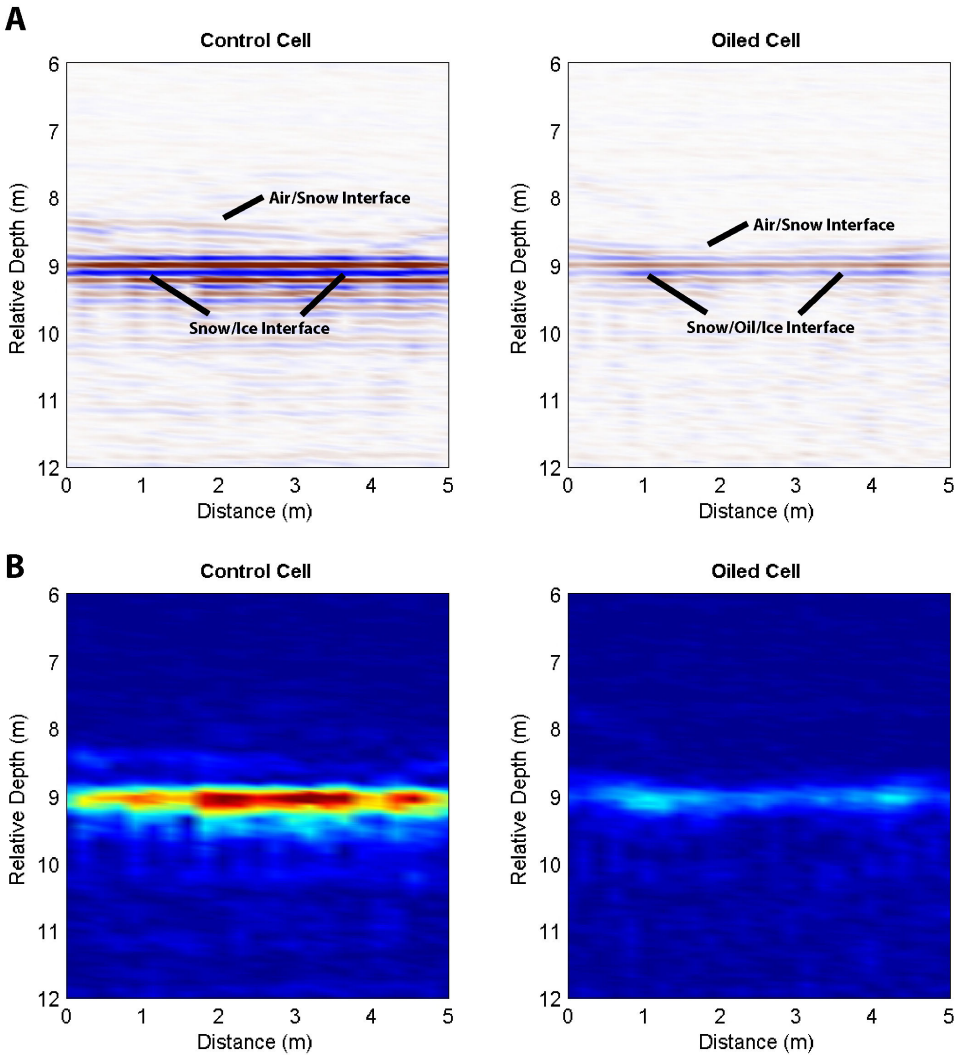

Figure 6-4 A) Plot of recorded GPR data acquired over the control and oiled cells at an altitude of 5m and speed of 5kt. B) Plot of reflection strength for the data shown in A. The reflection strength where the oil film is present is dramatically reduced relative to the control cell. This is consistent with numerical modeling results.

Similar results were obtained when the altitude was increased. Figure 6-5 shows the average amplitude and standard deviation of the ice interface reflection recorded at altitudes from 5 m to 20 m and speed of 5kt. The observed response was consistent at all altitudes and in all cases the mean of the control and oiled cells falls outside of measured uncertainty and are consistent with numerical predictions.

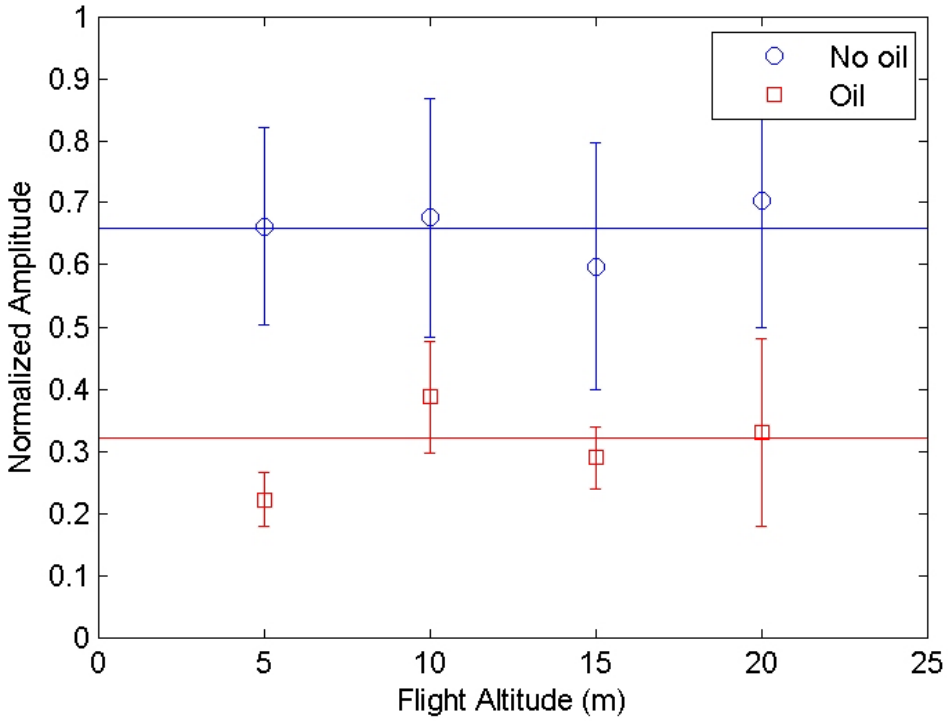

Figure 6-5 Summary of airborne radar results at speeds of 5N. The solid lines show the amplitudes predicted by numerical modeling. In all cases the mean amplitude of the oiled cell is significantly lower than that in the control cell.

Overall, this test indicates that GPR can readily detect oil spilled on the ice surface that is later buried by snow. Further, the results validate the numerical modeling approach that was used.

Scenario #2: Case study of oil penetration in snow

The configuration of oil and snow in this scenario was based on photograph of test trench with cold oil saturating snow in field trials documented in Mackay et al. (1974).

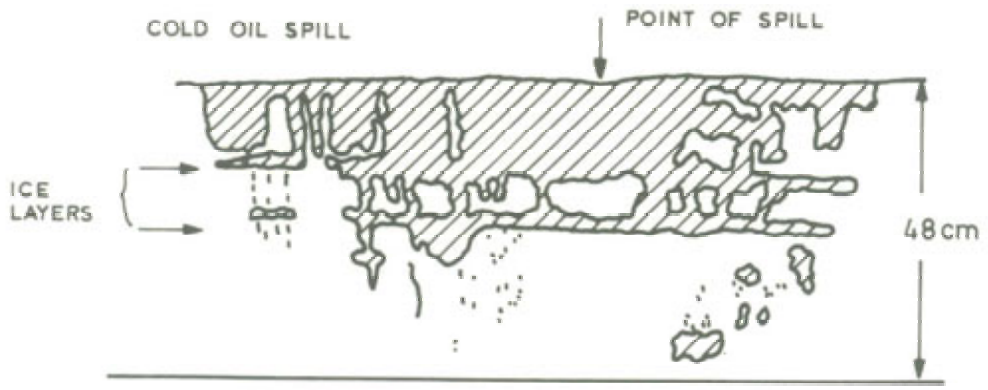

Figure 6-6 Diagram taken from McKay et al. (1974) illustrating the distribution of oil in the snow pack after a controlled spill used to define Scenario 2

Considerations

For this scenario, the oil in snow cross section (Figure 6-6 above) was digitized to produce a binary electric property model where darkened areas contained oil and white areas were oil free. A snow density of 0.35 g/cc and oil saturation of 50% was assumed for all oiled areas. Data were generated using the finite difference simulator.

Results

Fig. 6-7 shows the relative electrical permittivity distribution (on the left) with the radar response shown in Fig. - on the right. The air/snow reflector arrives at a traveltime of 3.9 ns and the snow/ice reflector occurs at 8 ns. The zone of oiled snow creates a complex pattern of scattered energy that is easily detectable at distances between 1 and 2 m and arrival times between 4 and 8 ns. These results clearly demonstrate that complex oil distributions within snow can generate a significant radar response.

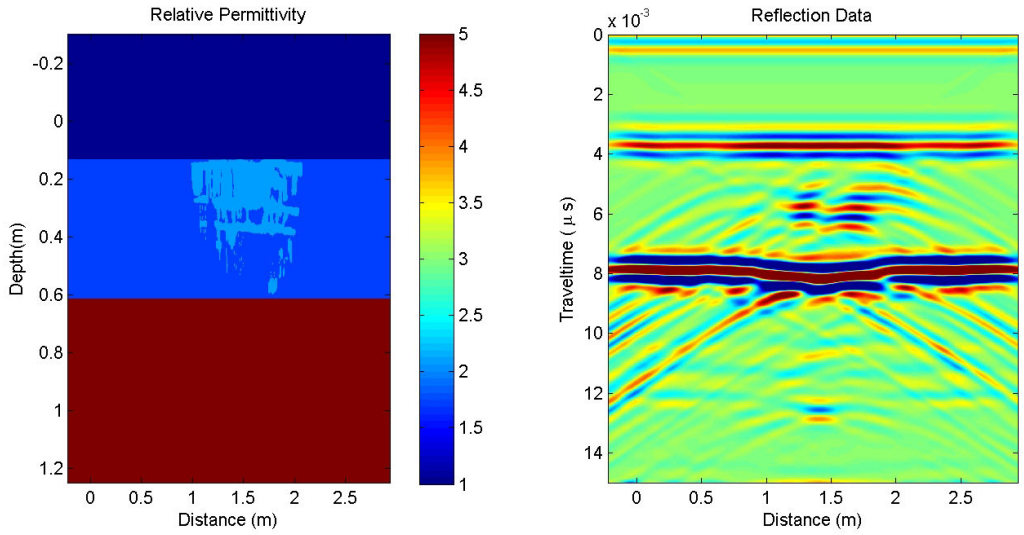

Figure 6-7 The relative permittivity model on the left was digitized from actual field measurements of oil distribution shown in Figure 6-6. Model GPR data on the right show a complex pattern of scattering caused by the presence of oil in the snow pack.

6.3.2 Ice and Oil Configurations

The following four scenarios cover a range of spill configurations involving lying in pools beneath a solid ice sheet and oil trapped or encapsulated as layers within the ice.

Scenario 3: 1D reflectivity modeling

The two main subsets of Scenario 3 presented below are:

- 3a - oil under ice
- 3b - oil layer trapped within the ice

The graphic representation shown as Fig. 6-8 for **Scenario 3a** shows the model of variable oil-under-ice layers increasing as the ice grows from November to April (based on the seasonal ice growth progression show earlier in Fig. 5-1). The under ice oil wedge varies from 0 to 20% of the ice thickness at any given time from November to April. We used 20% of the ice thickness as the maximum potential oil pool thickness, based on observations of natural first-year ice variability in the Canadian and US Beaufort Sea (Norcor 1977, Norcor 1975, Kovacs 1977, Barnes et al. 1979, Kovacs et al. 1981, Goodman et al. 1987).

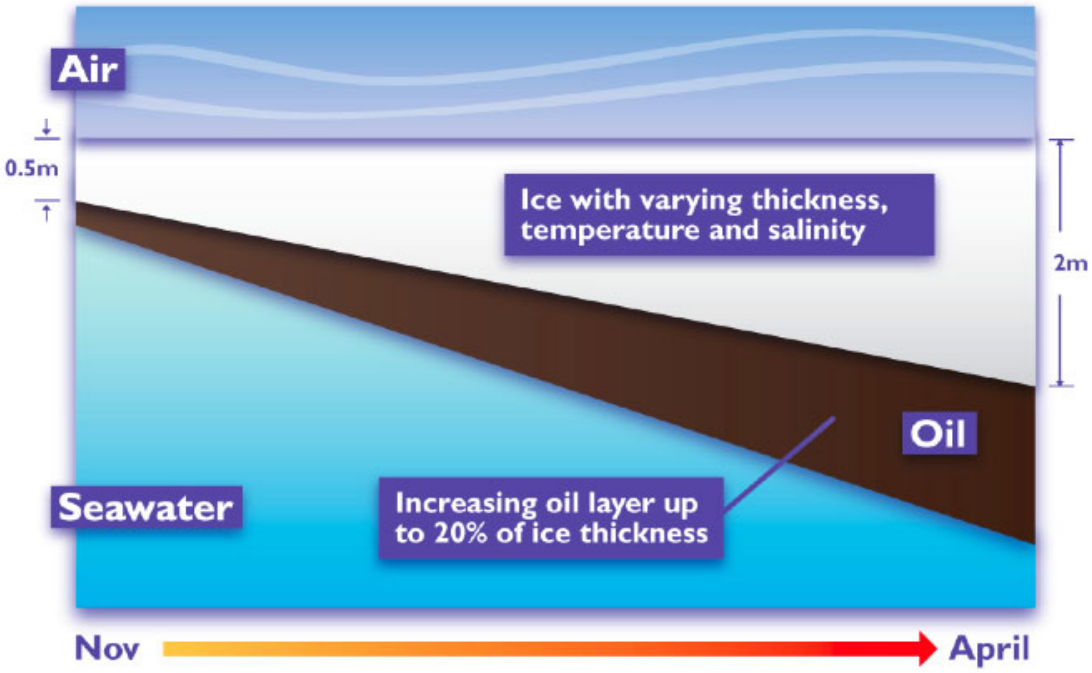

Figure 6-8 Scenario 3a - Oil Under Ice

Considerations

Scenario 3a (as well as 3b following) was run for each month covering the ice growth period from 30 cm in early November to a maximum of 2 m ice reached at the end of April. The main objective was to evaluate the effect of changing salinity and temperature profiles through the ice season (and therefore the electrical permittivity of the ice) on the radar signal response to a range of oil layer thickness under the ice. See background on oil and ice configurations and ice properties in Chapter 5.

Results

The following Fig. 6-9 shows the important ice properties varying with depth in the February time frame with no trapped oil as depicted in the sketch above.

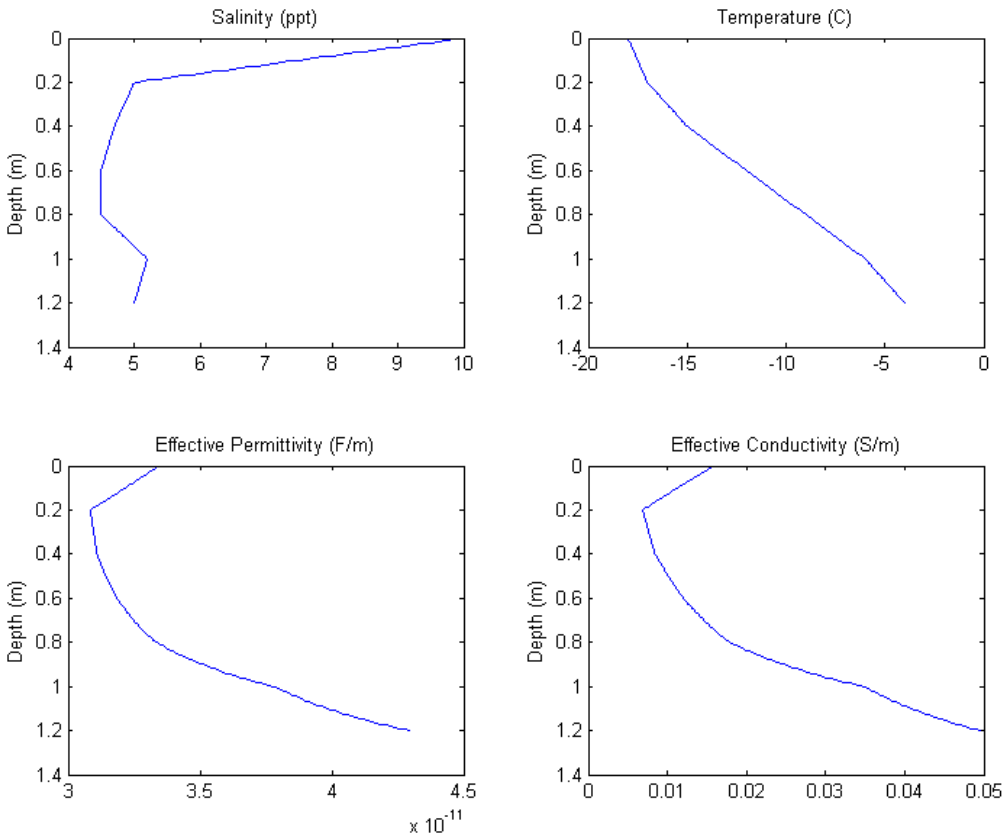

Figure 6-9 Ice property model with salinity and temperature profiles based on field measurements February field measurements in the Beaufort Sea. Electric property models are computed from the temperature and salinity profiles using the algorithm described in the text.

Figs. 6-10 and 6-11 show plots from the model output showing radar response to an under-ice oil layer varying in thickness within the ice as illustrated graphically in Fig. 6-8, presented as:

- Reflection image (what is recorded in the field with minimal processing)
- Amplitude (radar signal reflection strength)
- Instantaneous attributes

The oil layer varies from a minimum of 1 cm at the X-axis origin and increases to 20% of the total ice thickness (equivalent to 26 cm in February) at the far right of the X axis (10 m mark).

These results show that the GPR readily detected the oil layer beneath the ice throughout the winter period. A strong signal observed from the base of the ice and oil at the ice/water interface, produces amplitude, frequency and phase anomalies with oil thickness as thin as 1 cm. The amplitude anomaly (Fig. 6-11) is present across the full range of oil thickness, whereas the frequency and phase anomalies shown in the same figure are primarily sensitive to the oil where it thins to less than about 10 cm.

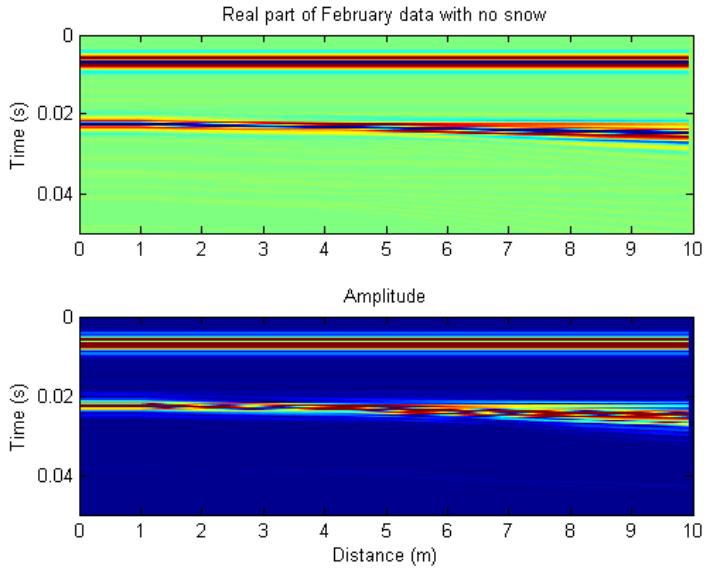

Figure 6-10 GPR data simulated using the 1D reflectivity model and reflection strength for varying oil thickness under typical February ice.

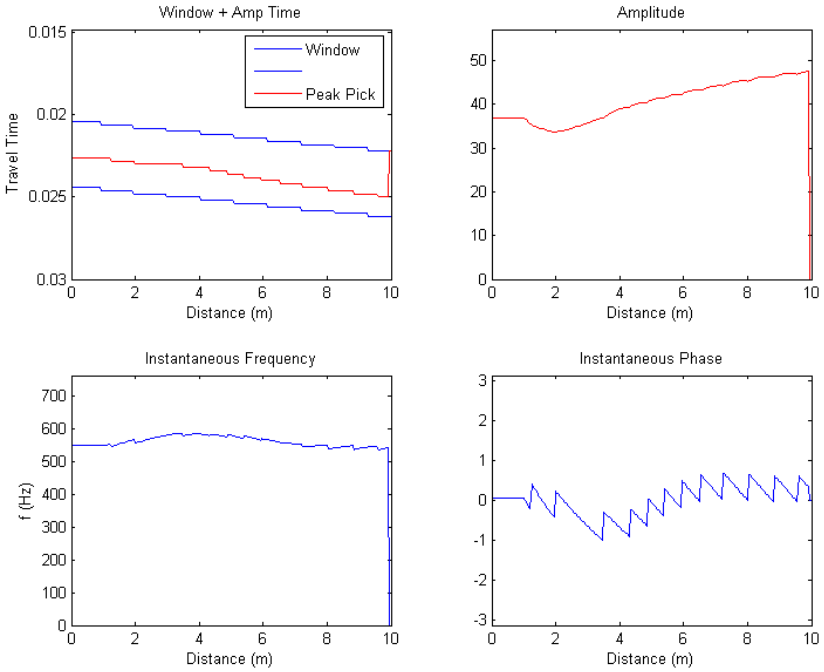

Figure 6-11 GPR reflection attributes taken from the data in Figure 6-10. The thin layer of oil produces a clear identifiable anomaly in all measurable attributes. Frequency and phase attributes return to the background values as the oil thickness approaches the conventional resolution of the GPR signal. The amplitude approaches a constant value that is higher than the background value.

Validation

The November model ice conditions are similar in terms of ice temperature, salinity and thickness, to the field experiments conducted at Svalbard in 2006 (65 cm of relatively warm ice). The modeled radar response for Nov (not shown here) is similar as well, especially the rate of signal attenuation. These findings tend to confirm the validity of the modeling tools being used in this study.

Results from the 2006 airborne tests over on Svalbard showed that the system was operating very close to the minimum acceptable signal to noise ratio at heights up to 20 m. We can use this analog to determine the additional power (relative to the existing commercial radar system) required to achieve oil under ice detection with warm, highly conductive ice sheets (represented by the Svea field trials). There is a critical temperature at around -5°C, above which the brine volume increase rapidly. This increase in brine volume results in a rapid increase in electric conductivity and prevents the radar signal from penetrating a significant thickness of ice. Early in the ice season ice (initial few weeks of growth), the negative aspects of the high brine volume are balanced by only having to penetrate relative thin ice. Consequently it is still possible to reach the oiled zone. However late season thick, warm ice will likely prevent the radar signal from reaching the target zone. In this model study, the ice/water interface and oil anomaly was detected for all cases, however for the May and October examples in particular, the signal is so weak that it would not likely be detected in field data.

Scenario 3b follows a similar approach to varying ice thickness, salinity and temperature and oil layer thickness with time only with the oil as trapped layers within the ice sheet at various depths. To create this scenario we inserted the conductivity and permittivity values for oil into the conductivity and permittivity curves for the sea ice. We assumed there was no change in salinity and temperature in the sea ice immediately above and below the entrapped oil layers (this effect was examined independently in Scenario 3c discussed later). See Fig. 6-12 for scenario illustration

Results

Fig. 6-13 below shows the variation in ice properties and permittivity and conductivity vs. depth for the case of multiple trapped oil layers in the ice sheet for the February example presented here. The trapped oil layers at 40, 80 and 1 m depths in the sheet create discontinuities in the permittivity and conductivity curves.

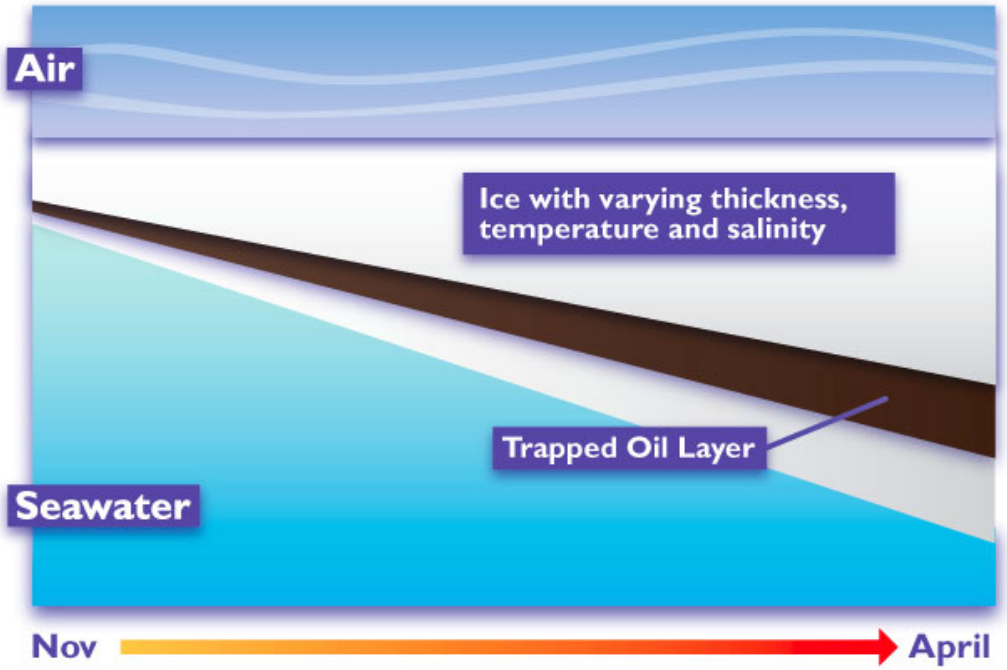

Figure 6-12 Scenario 3b - Oil trapped within the ice sheet. Illustration shows single trapped layer. Actual modeling inserted oil layers at 3 different depths.

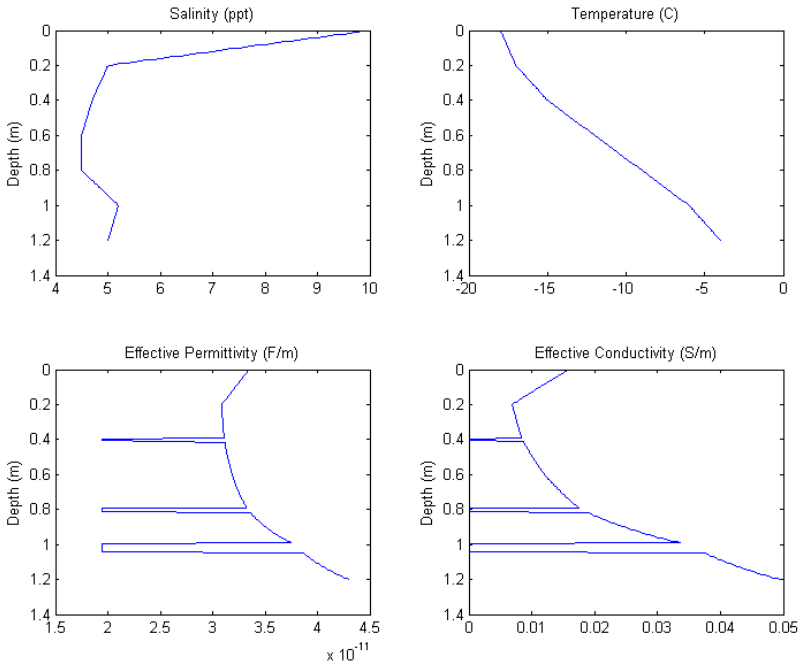

Figure 6-13 Material property models for February ice with thin layer of oil inserted at 0.4, 0.8 and 1 m depth.

Trapped thin oil layers within the ice produce identifiable reflections confirming cold basin results obtained at CRREL in 2004. The presence of the trapped oil appears to have little impact on the radar response from the ice/water interface (meaning that it is entirely possible to obtain an overall ice thickness profile at the same time as detecting oil within the ice).

Figs. 6-13 and 6-14 below show the: data profile, amplitude of reflection strength, and instantaneous attributes produced for the case of trapped oil layers in Scenario 3b.

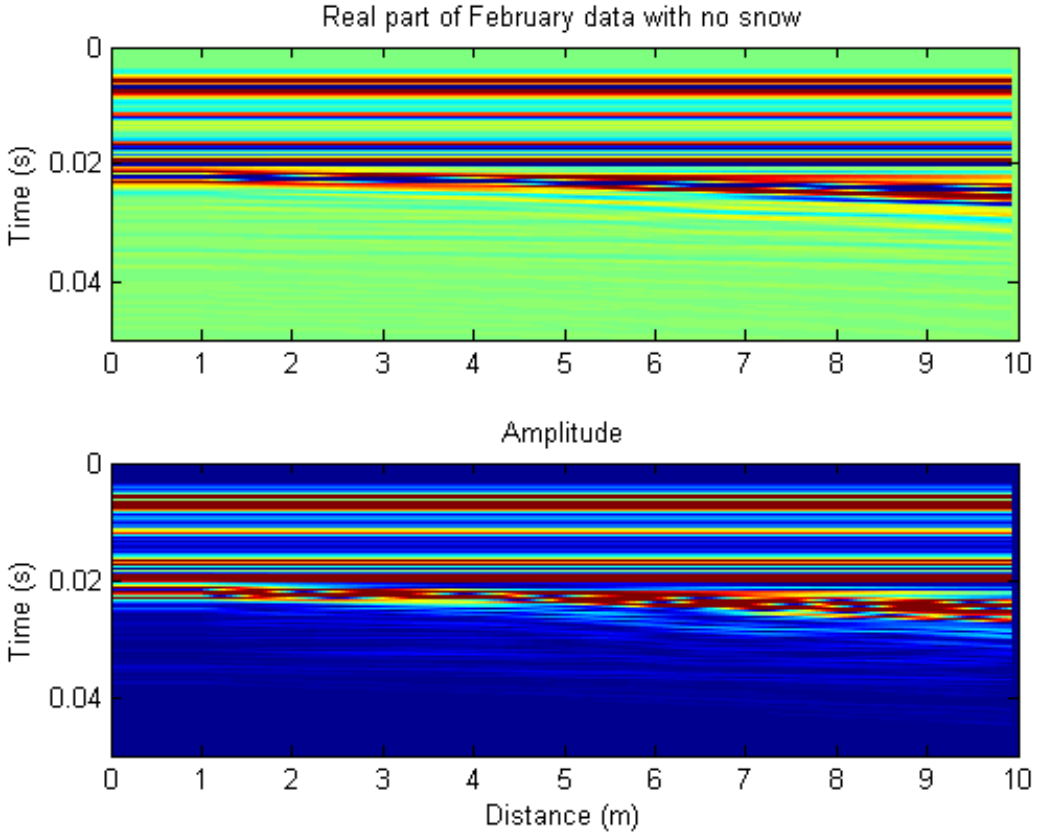

Figure 6-13 GPR data simulated with the 1D reflectivity model and measured reflection strength. Oil layers trapped within the ice produce distinct reflections.

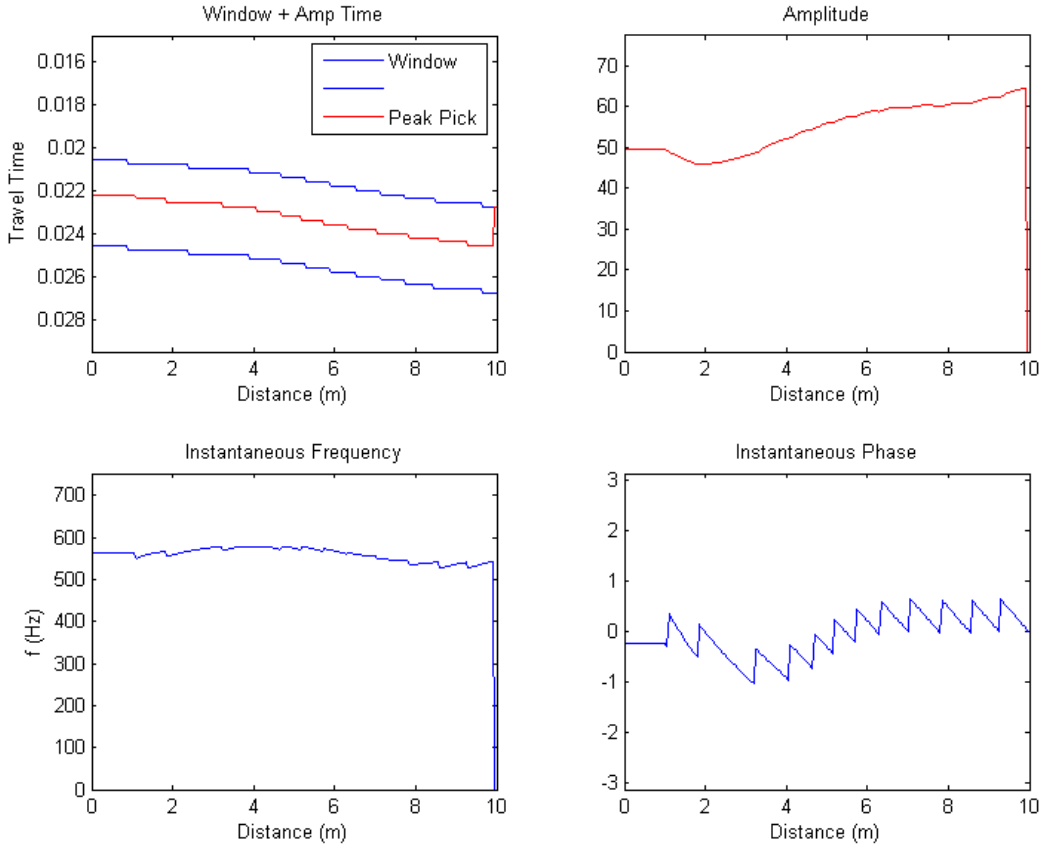

Figure 6-14 Attributes from the base of ice reflection when thin layers of oil are present within the ice. The thin layers do not have a significant effect on the base of ice reflection properties.

Subsets to Ice Scenario 3 (not illustrated)

Scenario 3c examines the effect of a jump in salinity noted in the historical Balaena Bay field experiment above and below trapped oil layers from cores extracted in early March (Norcor 1975). This effect was modeled for a single month using ice conditions representative of February. A one cm layer of oil was inserted at the mid-point in the ice sheet and the radar response modeled with the salinity anomaly found in field observations.

Result

The salinity anomaly had little impact on the signal response from the bottom of the ice, but the salinity anomaly together with the intraice oil layer produced an identifiable radar reflection from within the ice. The salinity increase above the oil did not degrade the radar signal appreciably.

Scenario 3 d examines the effect of varying snow depths in a single month (Feb) with constant air temperature. A linear temperature profile is assumed within the ice using a calculated value at the snow/ice interface to -1.8°C at the ice/water interface. The brine volume vs. depth in sheet was calculated using the expression described in Sanderson (1988) and presented earlier in Chapter 2. The temperature gradient through the snow layer was modeled after an analytical method described in Cammaert and Muggeridge (1988) based on a paper by Nakawo and Sinha (1981).

Using data for the month of February, we placed a snow layer that varied randomly between 10 and 20 cm thick above the ice and then calculated the snow depth-dependent ice temperature profile for each location. The oil layer thickness, ice thickness, and salinity profiles were based on the February case and utilized the oil under ice scenarios as described in Scenario 3a discussed earlier.

Results

Increasing snow depth in the range studied did result in an increase in ice temperature, but the radar still clearly images the base of the ice. However the variations in ice temperature for a variable thickness snow pack lead to variable attenuation of the radar signal. This variability causes significant variability in the amplitude response that is unrelated to the oil thickness, making interpretation more difficult.

However, the frequency and phase responses are independent of the snow depth, indicating that these attributes will likely be more robust indicators of the presence of oil in a field situation where varying snow thickness is the norm.

With snow thickness greater than 0.5 m, we found that the ice warms substantially and at snow depth of 1 m the ice had warmed enough to prevent effective radar signal penetration. Fortunately, snow depths of this magnitude are rarely found on level first-year sea ice in areas such as the Beaufort Sea. One exception would be local regions at the base of a pressure ridge along the upwind side. Ice in these areas is often depressed and partially flooded by the weight of overlying snow making radar surveys in these situations impractical. Sub-Arctic areas with marginal ice zones (Bering Sea for example) could experience much deeper snow covers on the ice. In that case, the presence of snow could impede radar surveys.

Scenario 4: 2-D Finite Difference - Constant sinusoidal variation in ice thickness

This set of scenarios adopts a sinusoidal variation in the ice-water boundary based on an original model presented in Norcor (1977). The sinusoid was generated with a 5 m wavelength and peak-trough height of 20 cm.

In all, five cases were considered in Scenario 4 (three are illustrated in the following sketches):

1) Smooth ice/water interface with no oil,
2) Rough ice/water interface with no oil,
3) Smooth ice/water interface with oil filling the peaks (illustrated in Fig. 6-15),
4) Same as 3, but with oil migrating some distance into the ice column creating a rough interface (illustrated in Fig. 6-16), and
5) Same as 4, but with a 2cm thick layer of oil trapped within the ice column and oil partially migrating upward through the ice (illustrated in Fig. 6-17).

The term *Smooth ice* here means that the boundary is a simple interface, whereas the *Rough* notation indicates that base of ice is irregular with either water (no oil case) or oil (oil cases) filling the irregularities. The irregular interfaces were constructed by introducing random vertical variation at the ice water interface between 0 and 12 cm. These variations occur over 2 – 3 mm laterally, which is comparable to the width of brine channels within natural sea ice.

All of the cases examined in this scenario use a typical ice thickness and ice internal properties representative of a February time frame (see Fig. 5-1 and Tables 5-2 and 5-3).

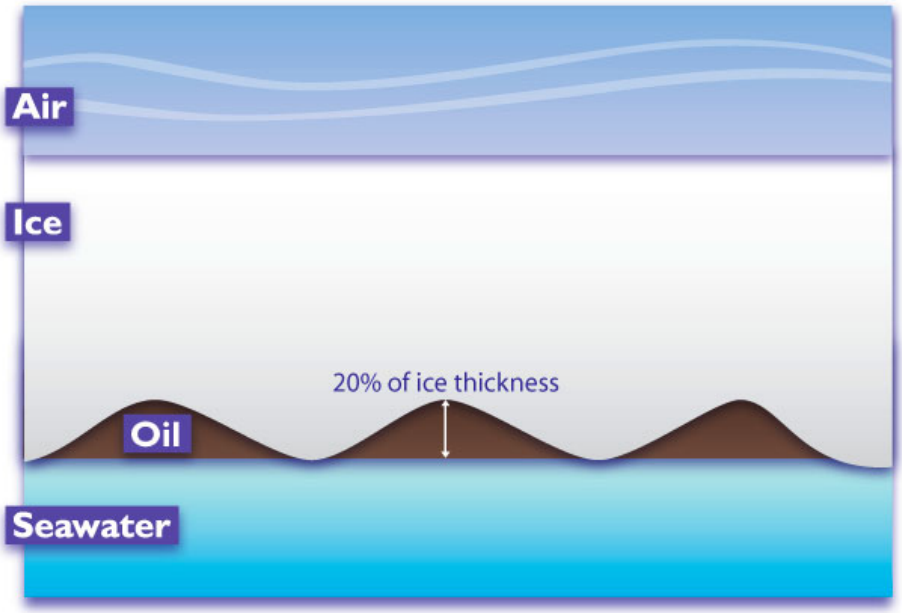

Figure 6-15 Scenario 4 Case #3 (also modeled as Case #1 without oil)

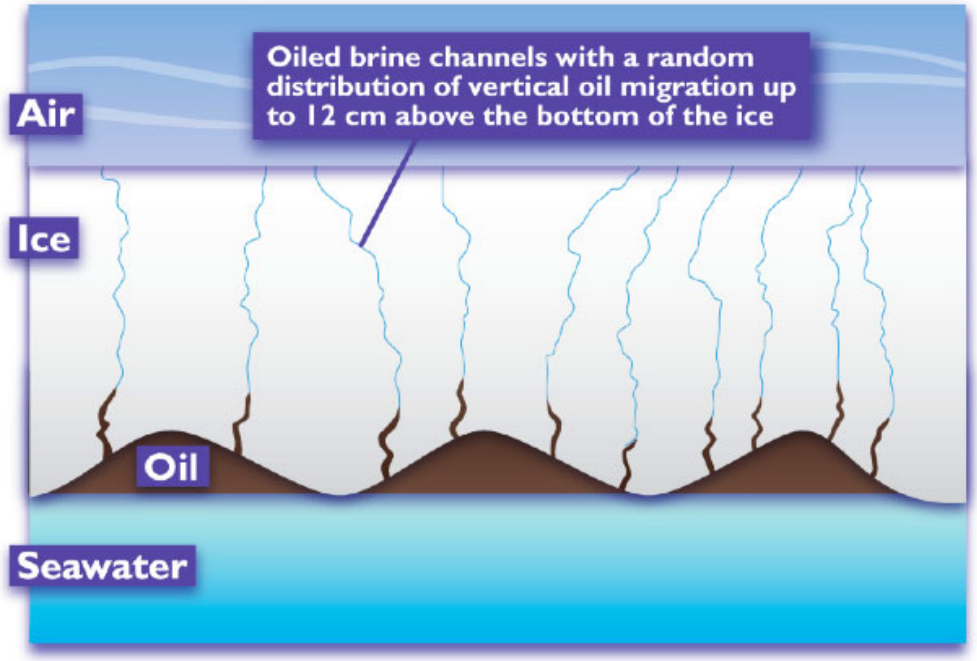

Figure 6-16 Scenario 4 Case #4

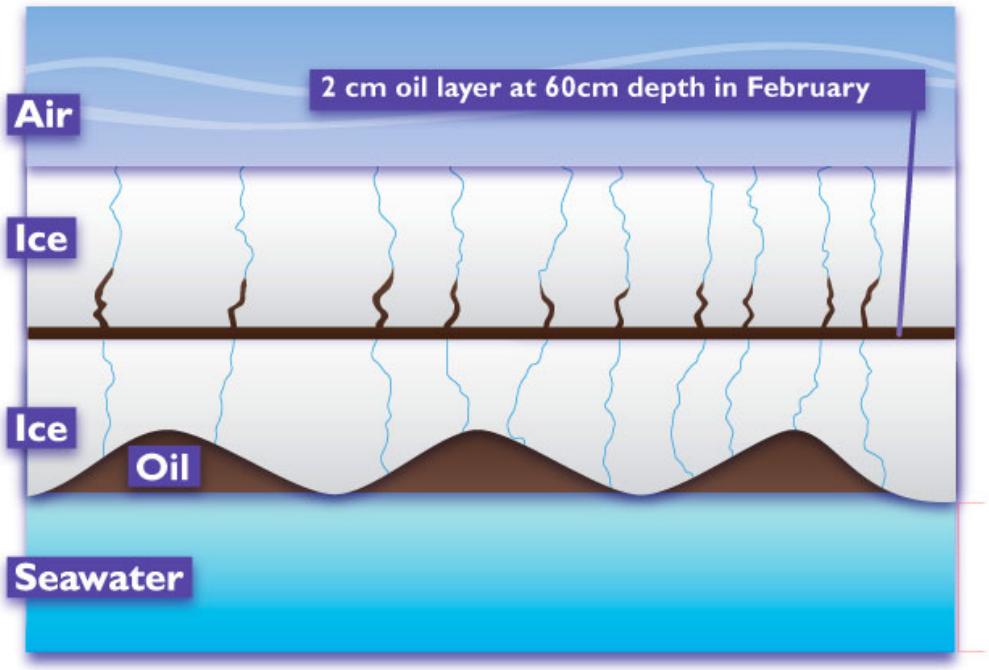

Figure 6-17 Scenario 4 Case #5

Results - no oil base case #1

Fig. 6-18 shows the electric permittivity and conductivity models along with the simulated GPR data for Scenario 4 Case #1 with no oil. In the GPR data, the reflection from the air/ice interface is present at a traveltime of just over 5 ns and the reflection from the base of the ice arrives at just over 15 ns. The sinusoidal shape of the base of the ice is evident in the radar data, however, because of scattering from the irregular surface, the GPR image gives a distorted picture of the actual subsurface topography. Additionally, high amplitudes (bright red spots) occur in the troughs because the radar signal becomes more focused in these areas, much like a satellite dish focuses electromagnetic waves incident from the atmosphere.

Fig. 6-19 below shows a plot of GPR reflection strength, frequency, and phase, at the water interface reflection for

Results in Fig. 6-19 shows that the reflection strength in all cases differs substantially as the oil thickens and thins, but that in the oiled cases, the variation is anti-correlated. The amplitude in the thick oil zones is much higher than the no oil case.

For the rough interface with no oil present, the amplitude is substantially lower and more variable than the smooth interface. Additionally, scattering interference causes a frequency downshift. Phase is largely unaffected by roughness at this scale. Both the phase and frequency are approximately constant for all cases in zones of thick oil.

Where the oil thins, significant anomalies in frequency and phase occur for both smooth and rough cases. Comparing the rough ice/water interface with no oil to the oiled case, the anomalies are substantially larger than for the smooth interface models. This result is consistent with field observations from both the CRREL test basin in 2004 and the oil under ice experiment conducted at Spitsbergen in 2006. It is important to note here to, that amplitude is a better indicator of oil in the thick oil zones, whereas the frequency and phase attributes are likely more robust in zones of thin oil that are below the conventional signal resolution. It is therefore important to utilize all attributes when deploying the GPR in an actual spill.

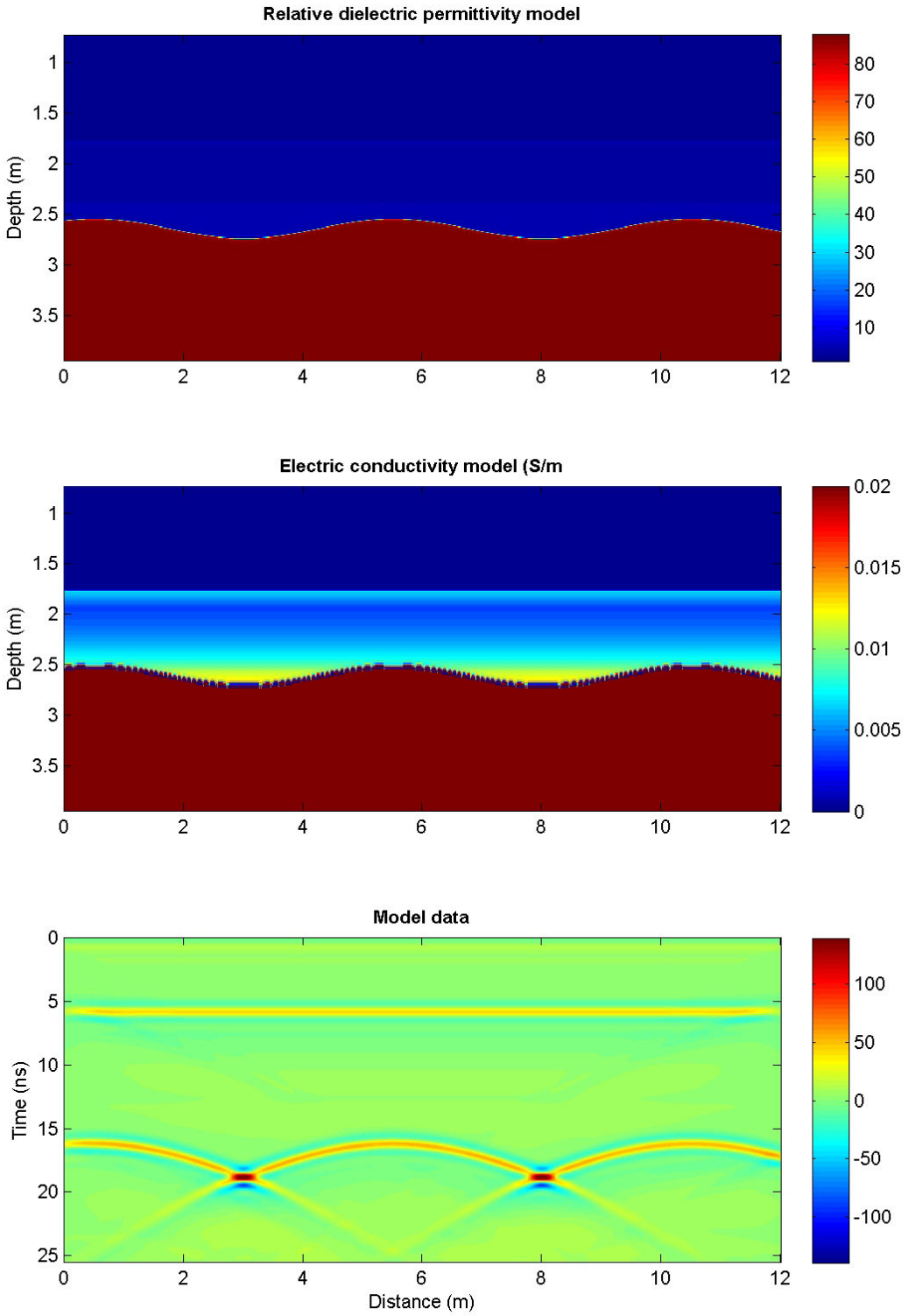

Figure 6-18 Electric property models and simulated GPR data for a laterally variable ice/water interface. The properties are based on our February test case used for Scenario 2

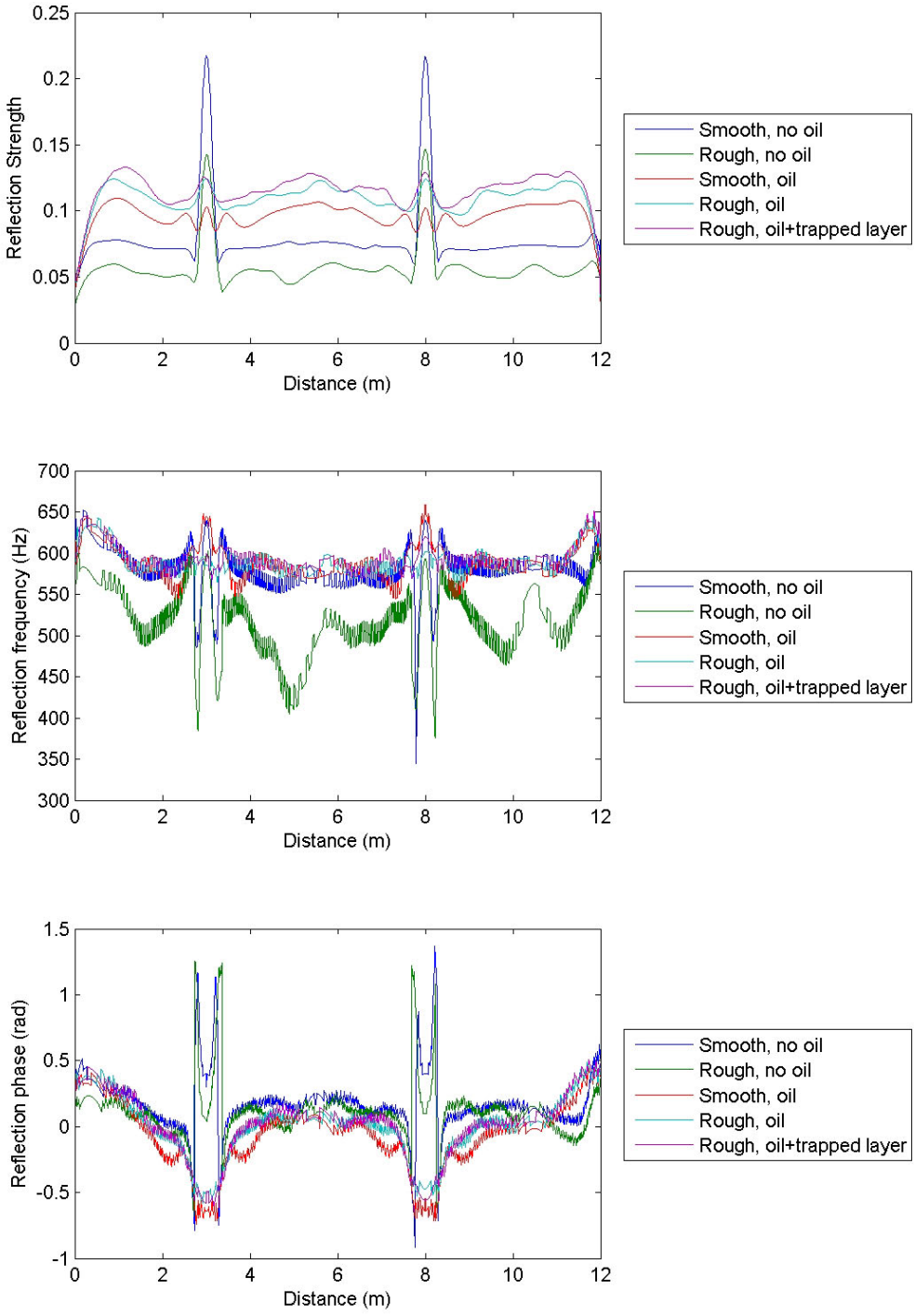

Figure 6-19 GPR reflection properties for a sinusoidally varying ice/water interface for simple smooth boundaries and with small-scale roughness present.

Scenario 5: 2-D Finite Difference - Decaying sinusoidal variation in ice thickness

This scenario examines the effect of varying the lateral and vertical dimensions of the oil pools under the ice by decaying the amplitude and wavelength of the under ice variations in thickness over a lateral dimension of 12 m. In the model simulation, the radar is deployed at elevations of 1 m (surface), and 15 and 30 m (helicopter). Again the ice conditions in February are used as the basis for the scenario (ice thickness, temperature and salinity).

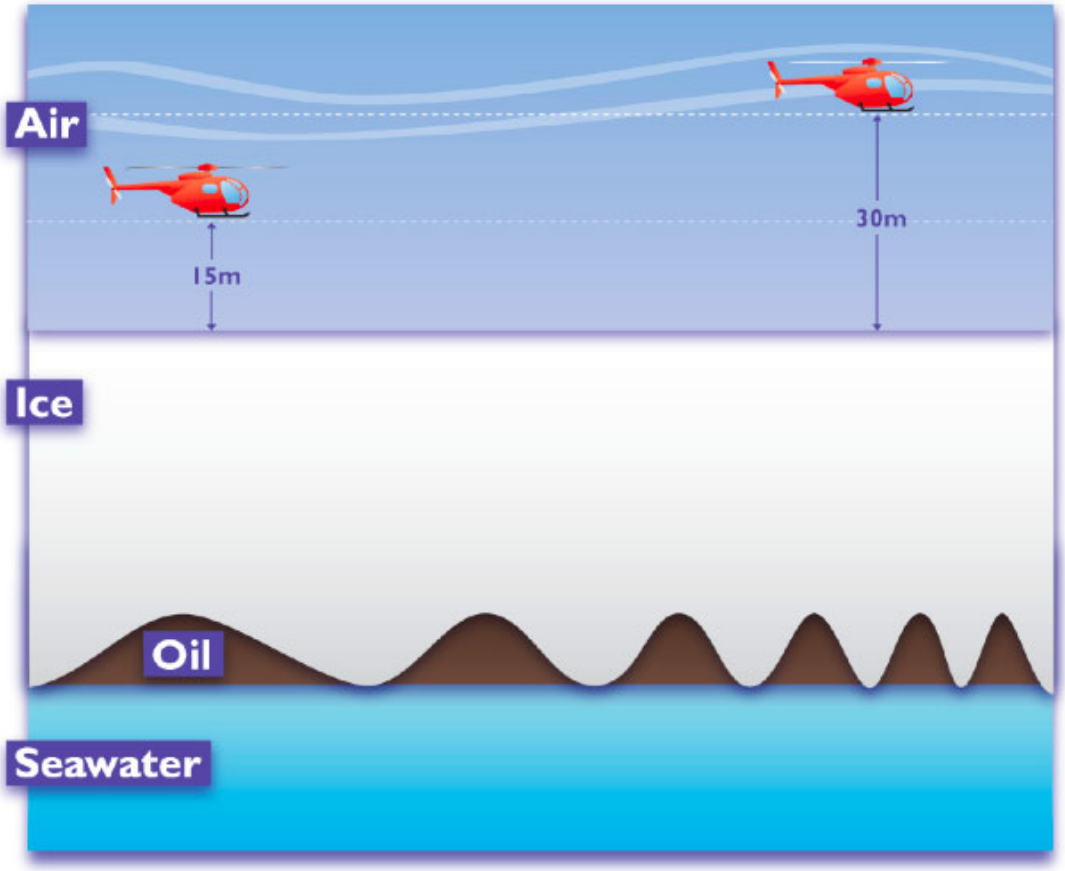

Figure 6-20 Scenario 5

Results

The oil/water interface was easily differentiable from the background response using the reflection strength attribute.

The plots below show the model outputs from this scenario for February.

Fig. 6-21 below shows the permittivity model and synthetic reflection data (antenna 1 m above the ice for the laterally varying sinusoidal ice/water interface with no oil present. The reflection data are complex showing scattering diffractions from the lateral discontinuities. It is clear that the lateral resolution decreases toward the right as the peaks become less distinct and diffractions are diminished.

Fig. 6-22below shows the properties of the reflected signal from the ice/water or ice/oil/water interface with and without oil present. Again the presence of oil causes an increase in reflection strength. The irregular amplitude is caused by interference associated with lateral scattering along the irregular interface. With increasing antenna height above the ice the relative amplitude increase caused by oil is not altered. However, the lateral variability in the reflection amplitude is smoothed because the signal is less sensitive to small-scale lateral changes. While the phase and frequency attributes show very complicated patterns, we see that they again converge where the oil is thick, and diverge where the oil is thin.

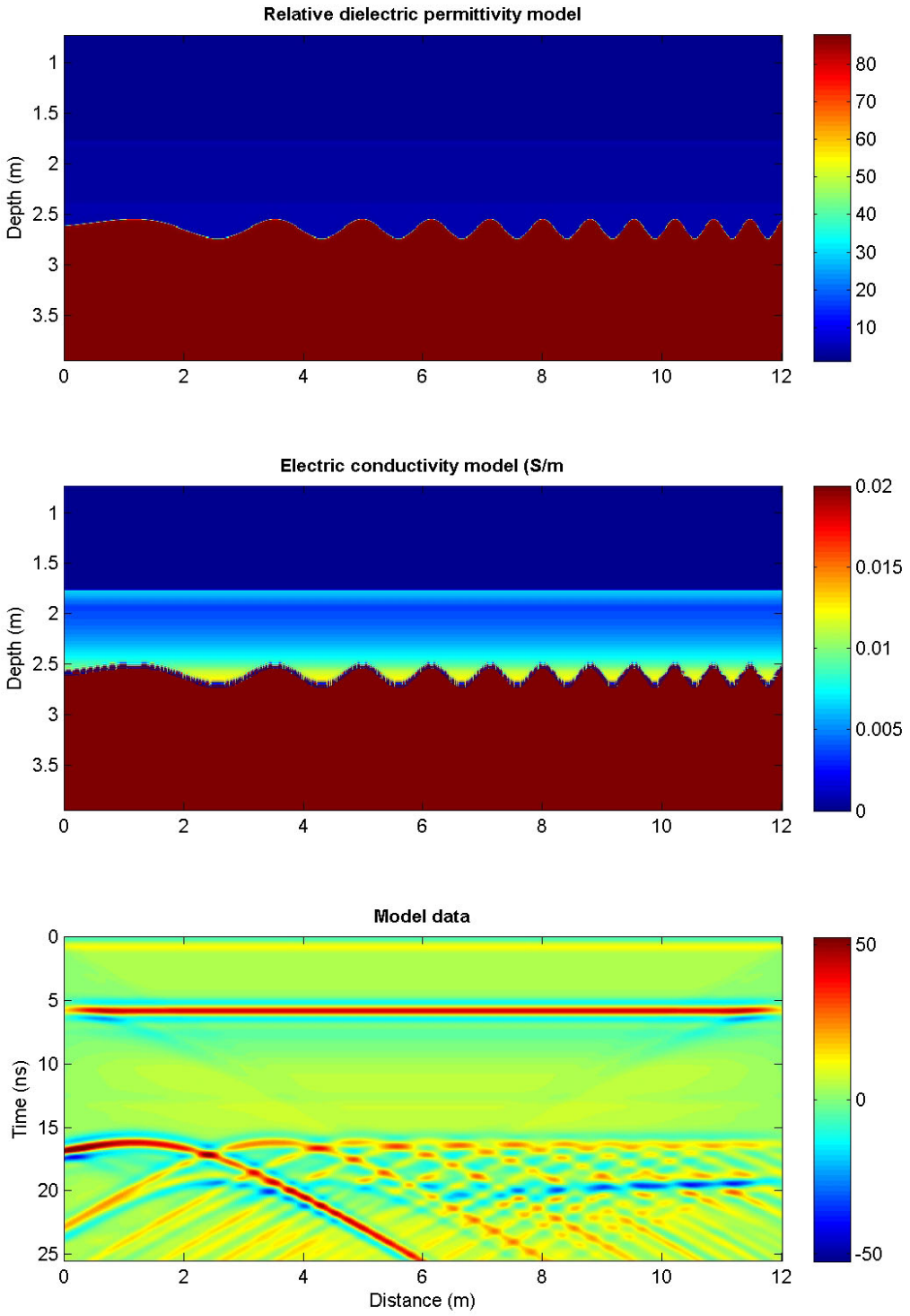

Figure 6-21 Electric property models for the case of an ice/water interface with decreasing sinusoid width toward the left. Model GPR data show a complex pattern of scattering. As the width of the anomalies decreases toward the left, the loss in lateral GPR resolution is evident.

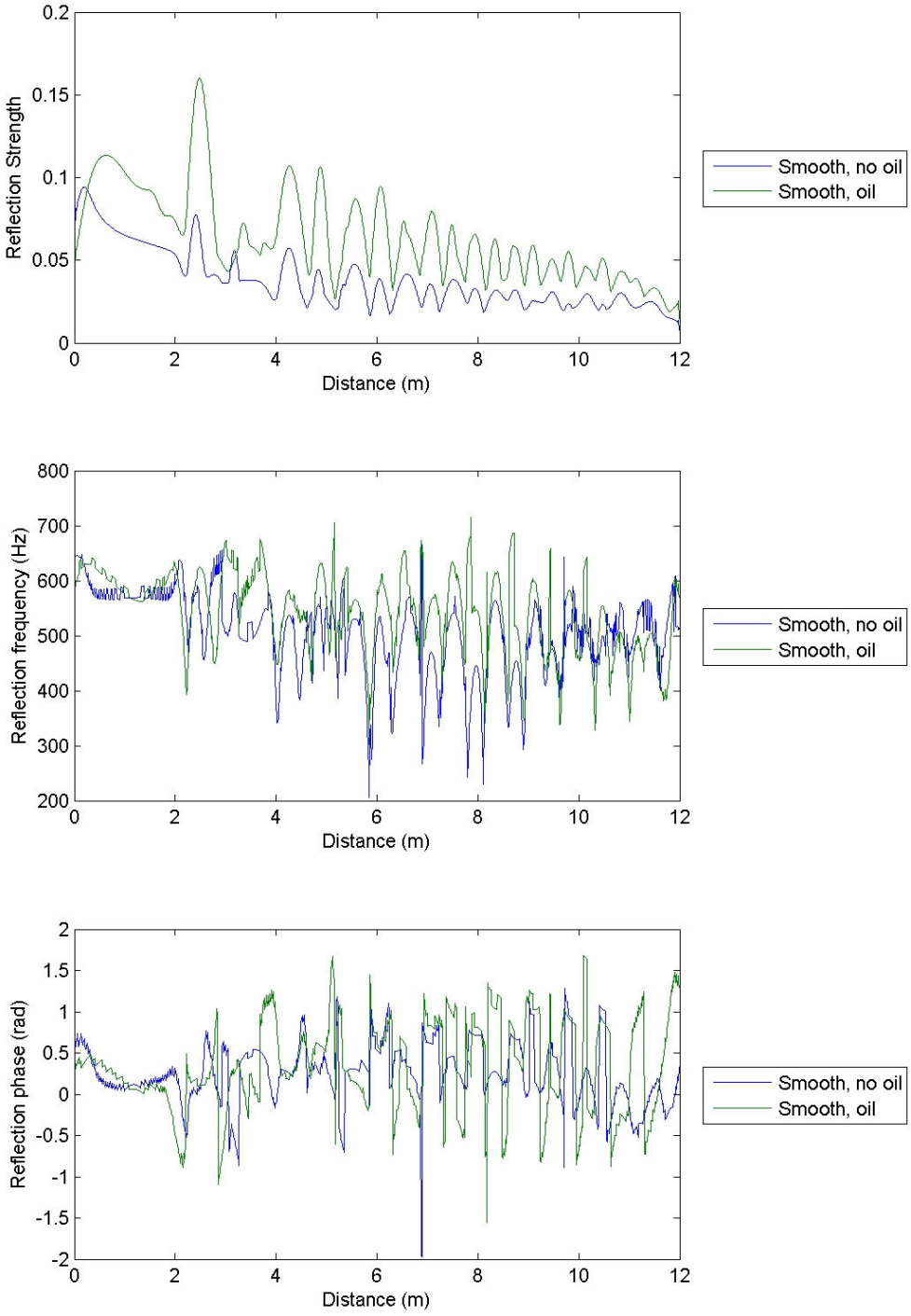

Figure 6-22 GPR reflection properties for the decaying sinusoid model. The attributes are complex, but again we find a substantial and detectable increase in reflection strength when the oil is present.

Scenario 6: Chronic Undetected Pipeline Leak

Scenario 6 examines the case of a slow leak from a submerged pipeline beneath stable fast ice (ice not moving). The leak rate is assumed to be below detectable limits (typically ~ 0.5 to 1% of flow). The resulting oil distribution over a period of weeks becomes a large pool of oily slush encased in ice on the top and sides but free to the water column below. This scenario was originally created by Dickins Associates as part of the oil spill information documents submitted during the EIS process for BP's Northstar development.

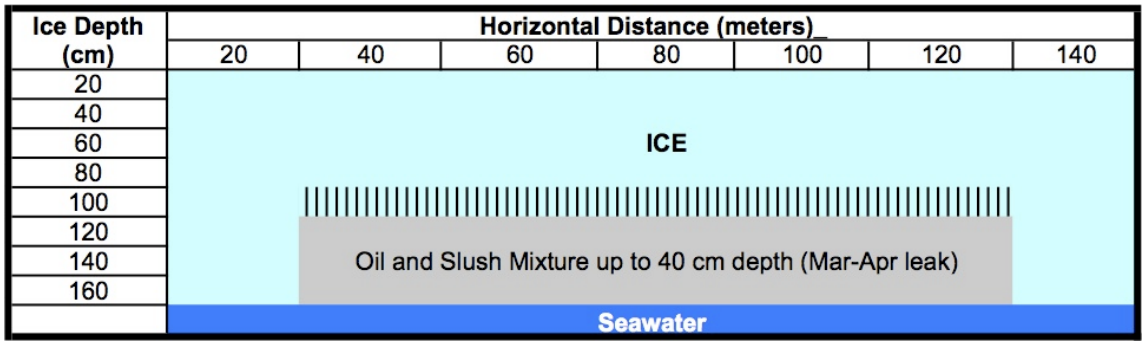

Figure 6-23 Scenario 6

For this model, the February representative [JHB2]profiles were used for ice properties. A 50% oil/ice mixture was assumed with 12 cm of oil migration into the brine channels above the oiled zone (shown as vertical bars in the sketch). This model produced a substantial GPR reflectivity anomaly and the oil was easily detectable as shown in Fig. 6-24.

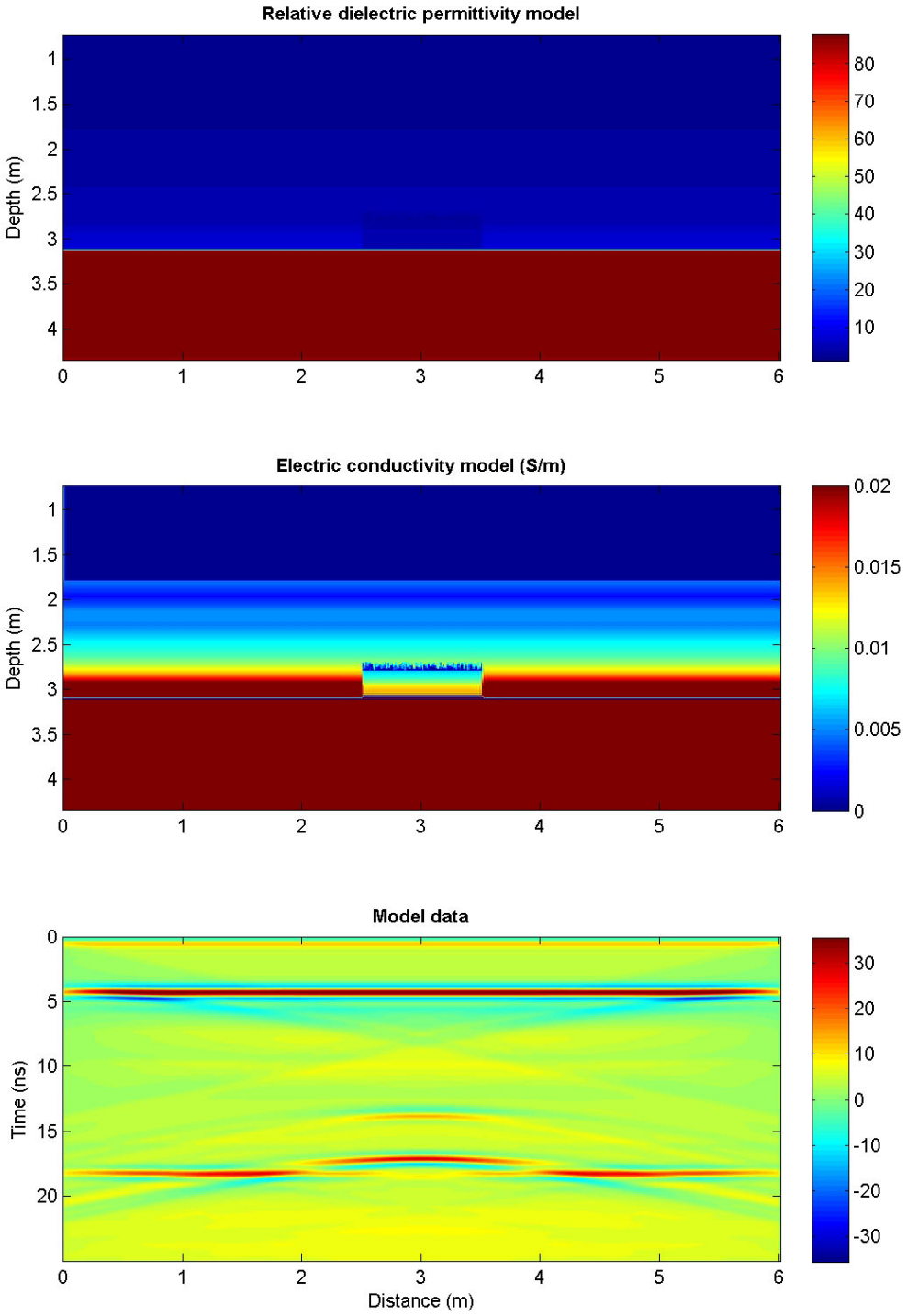

Figure 6-24 Electric property models and GPR simulation for the case of a chronic leaking pipe. The zone of oily slush is clearly identifiable between distances of 2 and 4 m in the GPR reflection image.

7. References and Bibliography

Barnes, P.W., E. Reimnitz, L. Toimil, and H. Hill. 1979. Fast Ice Thickness and Snow Depth in Relation to Oil Entrapment Potential, Prudhoe Bay, Alaska. USCG Open File Report 79-539, Menlo Park, CA.

Bech, C. and P. Sveum. 1991. Spreading of Oil in Snow. Proceedings of the Fourteenth Arctic and Marine Oilspill Program Technical Seminar, pp 57-71. 1991.

Belore, R.C. and I.A. Buist. 1988. Modeling of Oil Spills in Snow. Proceedings of the Eleventh Arctic and Marine Oilspill Program Technical Seminar, pp 9-29.

Best, H., McNamara, J.P. and Liberty, L., in review. Association of ice and river channel morphology determined using ground penetrating radar in the Kuparuk River, Alaska. Arctic, Antarctic, and Alpine Research, 37(2): 157-162.

Bradford, J.H., 2007. Frequency dependent attenuation analysis of ground-penetrating radar data. Geophysics, 72: J7-J16.

Bradford, J.H. July 2005. Task 4 Technical Note: GPR Software Development. Report by DF Dickins Associates Ltd. and Boise State University to the Minerals Management Service, Herndon, VA (Contract No. 0105PO39137).

Bradford, J.H. and Wu, Y., 2007. Instantaneous spectral analysis: Time-frequency mapping via wavelet matching with application to 3D GPR contaminated site characterization. The Leading Edge, 26: 1018-1023.

Bradford, J.H. and Deeds, J.C., 2006. Ground-penetrating radar theory and application of thinbed offset dependent reflectivity. Geophysics, 71(3): K47-K57.

Bradford J.H., Liberty L.M, and Dickins D.F. 2005. Oil Exploration at less than 2 M Depth: Instantaneous Attribute Analysis of Ground-Penetrating Radar Data for Detection of Crude Oil Under Sea Ice. SEG Technical Program Expanded Abstracts, pp. 1113-1116.

Brandvik, P.J., Faksness L-G, Dickins D.F. and Bradford J.H. Weathering of Oil Spills Under Arctic Conditions - Field Experiments with Different Ice Conditions Followed by In-Situ Burning. Presentation at NATO/CCMS third workshop on Oil Spill Response, Halifax, Nova Scotia, October 2006.

Brosten, T.R. et al., 2006. Profiles of temporal thaw depths beneath two arctic stream types using ground-penetrating radar. Permafrost and Periglacial Processes, 17: 341-355.

Butt, K., O'Reilly, P. and E. Reimer. 1981. A Field Evaluation of Impulse Radar for Detecting Oil in and Under Sea Ice. C-CORE, St. John's, 1981 (Appendix K to Vol II of the Oil and Gas Under Sea Ice Experiment, Dickins and Buist (1981), APOA Contract Report 169, Calgary, AB.

Cammaert, A.B., and D.B. Muggeridge. 1988. Ice Interaction with Offshore Structures. Van Nostrand, ISBN 0-442-21652-1, NY.

Cardimona, S. 2002. Subsurface Investigation Using Ground Penetrating Radar. Proceedings 2nd Annual Conference on the Application of Geophysical and NDT Methodologies to Transportation Facilities and Infrastructure, Rolla, MO.

Comfort, G., Roots, T, Chabot, L. and F. Abbott. 1983. Oil Behaviour Under Multi-year Ice at Griper By, NWT. Proceedings 6th Arctic and Marine Oilspill Program Technical Seminar, Environment Canada, Ottawa.

Cox, G.F. and W.F. Weeks. 1982. Equations for Determining the Gas and Brine Volumes of Sea Ice Samples. CRREL Report No. 83-23, Hanover NH.

Dickins, D.F. 2004. Advancing Oil Spill Response in Ice Covered Areas. Report submitted to the Prince William Sound Oil Spill Recovery Institute and US Arctic Research Commission, Cordova Alaska and Washington DC.

Dickins, D.F. October 2000. Detection and Tracking of Oil Under Ice. Final report submitted by DF Dickins Associates Ltd. to Minerals Management Service, Herndon VA.

Dickins D.F., Vaudrey K. and S. Potter. 2000. Oil Spills in Ice Discussion Paper: A Review of Spill Response, Ice Conditions, Oil Behavior and Monitoring, prepared by DF Dickins Associates Ltd., Vaudrey & Associates Inc., and SL Ross Environmental Research Limited for Alaska Clean Seas, Prudhoe Bay, AK.

Dickins, D. F., Brandvik, P.J., Faksness, L.-G., Bradford, J., and L. Liberty. 2006. Svalbard Experimental Spill to Study Spill Detection and Oil Behavior in Ice. Report prepared for MMS and sponsors by DF Dickins Associates Ltd., SINTEF, The University Centre in Svalbard, and Boise State University, Washington DC and Trondheim, Norway.

Dickins, D., Liberty L., Hirst W., Bradford J., Jones V., Zabilansky L., G. Gibson G., and J. Lane. 2005. New and Innovative Equipment and Technologies for the Remote Sensing and Surveillance of Oil in and Under Ice. Proceedings 28 th Arctic and Marine Oilspill Program Technical Seminar, Calgary, June 2005. (MMS Contract 1435-01-04-36285)

Dickins, D.F. and J. Bradford. July 2005. Field Testing GPR over a Variety of Sea Ice Conditions at Prudhoe Bay, Alaska April 18-20, 2005. Field report submitted by DF Dickins Associates Ltd. and Boise State University to the Minerals Management Service, Herndon, VA (Contract No. 0105PO39137).

Dickins, D. and I. Buist. 1999.Oil Spill Countermeasures for Ice Covered Waters. Journal of Pure and Applied Chemistry, Vol. 71, No 1, London, 1999.

Dickins, D.F., Buist, I.A., and W.M. Pistruzak. 1981. Dome Petroleum's Study of Oil and Gas Under Sea Ice. Proceedings International Oil Spill Conference, American Petroleum Institute, Wash. D.C., pp 183-189. (Full report in 2 Vols. cited in text as Dickins and Buist, 1981)

Frankenstein, G. and R. Garner. 1967. Equations for Determining the Brine Volume of Sea ice from -0.5° to -22.9°C. Journal of Glaciology 6*(48*), 943-944.

Goodman, R.H., Holoboff, A.G., Daley, W., Waddell, P., Murdock, L.D. and M. Fingas. 1987. A Technique for the Measurement of Under-Ice Roughness to Determine Oil Storage Volumes. Proceedings 10th International Oil Spill Conference, American Petroleum Institute.

Goodman, R., Jones, H., and M. Fingas. 1985. The Detection of Oil Under Ice Using Acoustics, Proc. Vol.2 of the Conference on Port and Ocean Engineering Under Arctic Conditions (POAC), Narssarssuaq, Greenland, pp. 903-916.

Harper, J.T. and Bradford, J.H., 2003. Snow stratigraphy over a uniform depositional surface: Spatial variability and measurement tools. *Cold Regions Science and Technology*.

Jones, H.W., and H.W. Kwan. 1982. The Detection of Oil Spills Under Arctic Ice by Ultrasound, Proc. 5th Annual Arctic Marine Oil Spill Program Technical Seminar, Environmental Protection Service, Ottawa, ON, pp. 391-411.

Kovacs, A., 1996. Sea Ice Part 1. Bulk Salinity vs. Ice Floe Thickness. CRREL Report 96-7, Hanover NH.

Kovacs, A. 1977. Sea Ice Thickness Profiling and and Under-Ice Oil Entrapment. Paper 2949. Proceedings 9th Annual Offshore Technology Conference, Houston.

Kovacs, A., R.M. Morey, D.F. Cundy, and G. Decoff. 1981. Pooling of Oil Under Sea Ice. Proceedings, POAC 81: Sixth International Conference on Port and Ocean Engineering under Arctic Conditions, Quebec, pp 912-922.

Løset, S., Singsaas, I., Sveum, P., Brandvik, P.J., and H. Jensen. 1994. Oljevern i nordlige og arktiske farvann (ONA) - Status: Volum I and II. STF60 F94087.

Mackay, D., 1974. Absorption and flow of oil into snow. In: "The Physical Aspects of Crude Oil Spills on Northern Terrain", ed. D. Mackay, M.E. Charles, and C.R. Phillips, Department of Indian and Northern Affairs, Task Force on Northern Development Report No. 73-42, Ottawa ON, 98-151.

Mackay, D., P. Leinonen, J. Overall, and B. Wood. 1975. The Behavior of Oil Spilled on Snow. in journal Arctic 28(1), pp 9-20.

McMinn, LTJG T.J. 1972. Crude Oil Behavior on Arctic Winter Ice: Final Report. Office of Research and Development, United States Coast Guard, Project 734108, Wash. D.C., NTIS Publication No. AP-754, 261 p.

Morey, R.M., Kovacs, A., and Cox, G.F.N., 1984, Electromagnetic properties of sea ice: Cold Regions Science and Technology, 9, 53-75.

Nakawo, M. and N.K. Sinha. 1981. Growth Rate and Salinity Profile of First-year Ice in the High Arctic. J. Glaciology, **27**(96), 315-330.

Nelson, W.G. and A.A. Allen. 1982. The Physical Interaction and Cleanup of Crude Oil with Slush and Solid First Year Ice. Proceedings of the Fifth Arctic Marine Oil Spill Program Technical Seminar, 1982, pp 37-59.

Norcor Engineering. 1977. Probable Behaviour and Fate of a Winter Spill in the Beaufort Sea. For Department of Fisheries and Environment Canada. Rept. No. EPS 4-EC-77-5

NORCOR Engineering and Research Ltd. 1975. The Interaction of Crude Oil with Arctic Sea Ice. Beaufort Sea Project Technical Report No. 27, Canada Department of the Environment, Victoria, British Columbia.

Nyland, D., 2004. Profiles of floating ice in Arctic regions using GPR, The Leading Edge, pp. 665-668.

Orlando, L., 2002. Detection and analysis of LNAPL using the instantaneous amplitude and frequency of ground-penetrating radar data. Geophysical Prospecting, 50: 27-41.

Owens, E.H., Dickins, D.F. and G.A. Sergy. 2005. The Behavior And Documentation Of Oil Spilled On Snow- And Ice-Covered Shorelines. Proceedings International Oil Spill Conference, Miami.

Rigor, I.G. and J.M. Wallace. 2004. Variations in the Age of Sea Ice and Summer Sea Ice Extent, Geophys. Res. Lett., v. 31, doi :10.1029 /2004GL019492.

Sanderson, T.J. 1988. Ice Mechanics: Risks to Offshore Structures. Graham and Totman, London.

Sheriff, R.E. 2002. Encyclopedic Dictionary of Applied Geophysics, Fourth Edition. Society of Exploration Geophysicists, 323 p.

SL Ross Environmental Research Ltd. and DF Dickins Associates Ltd. 1988. Modelling of Oil Spills in Snow. Environment Canada Report EE-109, River Road Laboratory, Ottawa ON, 69 pp.

Sorstrom, S-E. 2007. Joint Industry Arctic Oil Spill Research Program. International Oil and Ice Workshop, October 10-11, Anchorage AK.

Xie, Y. and Farmer, D.M., 1994, Seismic acoustic sensing of sea ice wave mechanical properties, *Journal of Geophysical Research*, Vol. 99, No. C4, p. 7771-7786 (93JC03483).

Zubov, N.N. 1945. Arctic Ice. Izdatel'stvo Glavsermorputi, Moscow. English translation by US Navy Oceanographic Office/American Meteorological Society.

The Department of the Interior Mission

As the Nation's principal conservation agency, the Department of the Interior has responsibility for most of our nationally owned public lands and natural resources. This includes fostering sound use of our land and water resources; protecting our fish, wildlife, and biological diversity; preserving the environmental and cultural values of our national parks and historical places; and providing for the enjoyment of life through outdoor recreation. The Department assesses our energy and mineral resources and works to ensure that their development is in the best interests of all our people by encouraging stewardship and citizen participation in their care. The Department also has a major responsibility for American Indian reservation communities and for people who live in island territories under U.S. administration.

The Minerals Management Service Mission

As a bureau of the Department of the Interior, the Minerals Management Service's (MMS) primary responsibilities are to manage the mineral resources located on the Nation's Outer Continental Shelf (OCS), collect revenue from the Federal OCS and onshore Federal and Indian lands, and distribute those revenues.

Moreover, in working to meet its responsibilities, the **Offshore Minerals Management Program** administers the OCS competitive leasing program and oversees the safe and environmentally sound exploration and production of our Nation's offshore natural gas, oil and other mineral resources. The MMS **Royalty Management Program** meets its responsibilities by ensuring the efficient, timely and accurate collection and disbursement of revenue from mineral leasing and production due to Indian tribes and allottees, States and the U.S. Treasury.

The MMS strives to fulfill its responsibilities through the general guiding principles of: (1) being responsive to the public's concerns and interests by maintaining a dialogue with all potentially affected parties and (2) carrying out its programs with an emphasis on working to enhance the quality of life for all Americans by lending MMS assistance and expertise to economic development and environmental protection.